Ryerson University
Digital Commons @ Ryerson

Theses and dissertations

1-1-2007

Experimental and finite element analysis of articular cartilage

Abdolreza Karami
Ryerson University

Follow this and additional works at: http://digitalcommons.ryerson.ca/dissertations

 Part of the Aerospace Engineering Commons

Recommended Citation
Karami, Abdolreza, "Experimental and finite element analysis of articular cartilage" (2007). *Theses and dissertations.* Paper 207.

This Thesis is brought to you for free and open access by Digital Commons @ Ryerson. It has been accepted for inclusion in Theses and dissertations by an authorized administrator of Digital Commons @ Ryerson. For more information, please contact bcameron@ryerson.ca.

619 .28

EXPERIMENTAL AND FINITE ELEMENT ANALYSIS OF ARTICULAR CARTILAGE

BY

ABDOLREZA KARAMI

Mechanical Engineering Department, Sharif University of Technology, Tehran, IRAN, 2004

A THESIS
PRESENTED TO RYERSON UNIVERSITY

in partial fulfillment of the
requirements for the degree of
Master of Applied Science
In the program of
Aerospace Engineering

Toronto, Ontario, Canada, 2007
Abdolreza Karami 2007 ©

PROPERTY OF
RYERSON UNIVERSITY LIBRARY

UMI Number: EC54200

INFORMATION TO USERS

The quality of this reproduction is dependent upon the quality of the copy submitted. Broken or indistinct print, colored or poor quality illustrations and photographs, print bleed-through, substandard margins, and improper alignment can adversely affect reproduction.

In the unlikely event that the author did not send a complete manuscript and there are missing pages, these will be noted. Also, if unauthorized copyright material had to be removed, a note will indicate the deletion.

UMI®

UMI Microform EC54200
Copyright 2009 by ProQuest LLC
All rights reserved. This microform edition is protected against unauthorized copying under Title 17, United States Code.

ProQuest LLC
789 East Eisenhower Parkway
P.O. Box 1346
Ann Arbor, MI 48106-1346

Abstract

Experimental and Finite Element Analysis of Articular Cartilage

Master of Applied Science, Aerospace Engineering, 2007, Abdolreza Karami

School of Graduate Studies, Ryerson University

In the clinical field, articular cartilage has an important role in performance of most joints in the human body. In the present study, articular cartilage was excised from the knee joint of a bovine and tested in a tensile testing machine. The data obtained from the test was used to calculate the material properties of the cartilage.

The material properties obtained from the experimental work were validated against the published experimental results in the literature. As the values from the experiment were in satisfactory agreement with the published data, it was concluded that the test protocol used in the experiment provides reliable data.

Next, the material properties were implemented in a finite element model of C3-C4 of cervical spine to examine if the finite element analysis can provide an accurate prediction of the behavior of the cervical spine. The stress and displacement results of the finite element analysis were consistent with the reported data in the literature. The location and the amount of the maximum stresses were examined and compared with the failure point of the materials.

Acknowledgment

I would like to express my deepest sense of gratitude to my supervisor Dr. Kamran Behdinan for his patient guidance, encouragement and excellent advice throughout this study.

I am thankful to Dr. Hamid Ghaemi for his generous assistance and advice during this time.

Table of Contents

List of Figures

List of Tables

1 Introduction

The cervical spine is one of the most important parts of the human body. This structure carries the majority of the loads on the body and the major movements of the body are controlled and affected by this part. This fact makes spinal disorders very serious and for this reason, movements or loads that can risk spinal health are studied by many researchers. The complicated and unique structure of the cervical spine inspires innovative research through a variety of methods to study the spine in order to find the causes of injuries to the spine and how to prevent them.

There have been distinctly different ways by which the cervical spine has been studied. These methods are normally used in the studies of other organs in the human body as well. Due to the exclusive anatomy of the cervical spine, some of them are more prevalent than the others.

In studying the human body, if an animal is used as the model, the assumption is the equivalence between the characteristics of the animal and human tissues. This sample is tested in a designed testing apparatus under controlled conditions and the values are measured during the experiment and the results are reported.

Clinical study is a method to study a live organ by means of statistical data or the data gathered by medical organizations from patients. This method is normally used in medical research.

An analytical approach is another method to study a system. Since live organs usually have complicated geometry and material properties, this method is rarely used by biomechanical engineers and a number of papers in biomechanics are published that are purely analytical (see [19]).

Numerical analysis is another method to study a model. In this method, the geometry is developed and material properties of the model are implemented and the initial and boundary conditions are applied to study the behavior of the model. The accuracy of the results is highly dependant on the accuracy of the geometry, material properties and boundary or initial conditions of the model. The Finite Element Method (FEM) is the numerical analysis method mostly used by biomechanical engineers to study the spine. This method enables the researcher to model the geometry, apply boundary conditions and material properties and obtain the stress and strain distribution. The choice of linearity or nonlinearity, static or dynamic and method of numeric solution are all decided by the researcher based on the results required and the limitations of simulation.

To carry out a finite element (FE) analysis one has to first create a model. The resemblance between the model and the real structure may have a very big effect on the

accuracy of the results. So researchers usually try to obtain an acceptable geometry of the model but because the geometries of live organs are so intricate and complicated, this stage becomes very challenging in the FE study of an organ. Usually, simplifications and some assumptions in geometry make this step more manageable without loss of accuracy. Once the model is created, the material properties are assigned. The material properties are always obtained from an experimental analysis on real tissue. The next step is to apply the initial and boundary conditions. The boundary conditions include the loads and the constraints on the model. After this step the model is solved.

The present study is concerned with the mechanical response of cervical spine and more specifically, on the vertebrae and discs. Therefore, the literature survey carried out in this study initially explains the anatomy of the cervical spine and especially intervertebral discs. Intervertebral disc was tested in an experiment later in this study, so it was highly noticed in the literature review. Vertebral units, ligaments and overall view of the cervical spine have been studied briefly as well.

The second part of the survey explains the experimental methods used to test the cartilage and the intervertebral discs. This part was a helpful step in selecting the proper test protocol suitable for our test specimen. Since the cartilage obtained from a bovine is used as a replacement for human intervertebral disc, the publications about testing animal cartilages were studied.

The next part of the literature survey is about the articles published regarding the FEM in analyzing the spine or vertebrae. The load conditions, the element choice, type of solution and the material properties used in these papers can be used to have a better FE model.

In all the above subjects, the results obtained from the presented study were compared to the results of the published data in the literature to examine the method used.

Tensile testing of soft tissues has always been one the most important parts of biomechanical studies. The stress increases much faster with increasing strain than Hooke's law predicts when testing animal tissue. Tissues in a physiological state are usually stressed. For example, lung tissue is in tension all the time. If a segment of artery is excited and tested in a tensile testing machine by imposing a cyclically varying strain, the stress response will show a loop with each cycle, but the loop decreases with succeeding cycles, rapidly at first, tending to a steady state after a number of cycles.

The existence of such an initial period of adjustment after a large disturbance seems common to all biological tissues. From the point of view of mechanical testing the process is called preconditioning.

In an experiment [1], tension was applied to a rabbit mesentary muscle by loading and unloading. It was seen that the loop did not depend very much on the rate of strain. This insensitivity with respect to the strain rate holds in a wide range of strain rate [1].

Figure 1. 1 shows a relaxation curve for rabbit mesentary. The specimen was strained at a constant rate until the maximum tension desired was obtained. The length of the specimen was then held constant and the change of tension with time was recorded [1].

For relaxation over a long period of time, in seventeen hours, a large portion of initial stress was relaxed [1].

The features of hysteresis, relaxation and creep at lower stress ranges can be seen in almost all different materials tested in the laboratory. The major differences among the tissues are capability of being stretched [1].

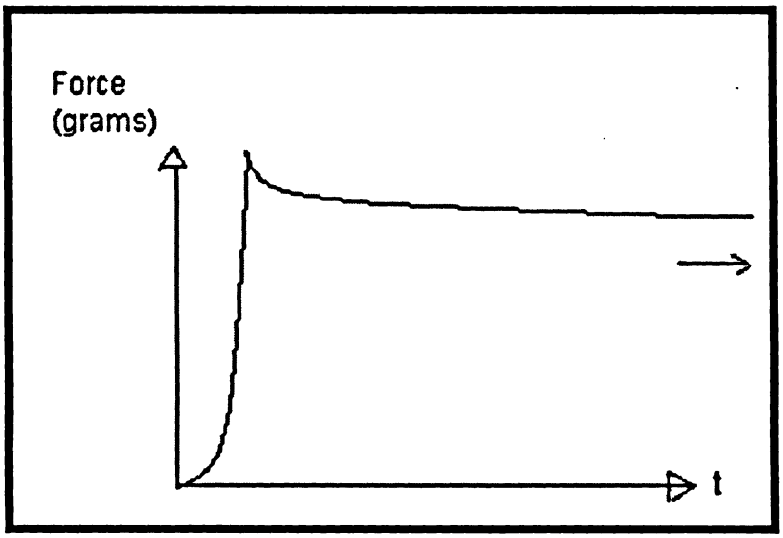

Figure 1. 1 Relaxation curve of rabbit mesentery [1]

In the physiological range, mesentery can be stretched about 100-200% from the relaxed length; the ureter can be stretched about 60%, the resting heart muscle about 15%, the arteries and veins about 60%. If stretched much more than these ranges, the tissues will fail and yield. This characteristic is more specific with different tissues [1].

Ligaments are uniaxial structures that carry only tensile forces. However, some ligaments are capable of resisting tensile forces in different directions because of their orientation and location. The anterior longitudinal ligament usually functions under an extension bending moment. Ligaments such as the posterior longitudinal ligament show less force resistance than the anterior longitudinal, because they are located close to the center of rotation. Ligaments are most effective when pulled along the direction of their fibers [2].

In order to investigate the role of spinal ligaments and to model cervical spine behavior, it is important to have their accurate geometry (origin, length and cross-sectional area) and material properties (stiffness, force-deflection, and stress-strain) [2].

From a mathematical modeling viewpoint, to create a model, fundamental properties such as stiffness or elastic modulus (or a function of stress and strain as mechanical property),

are generally required. These properties are obtained by testing the ligament in tensile loading. Experiments conducted with human cervical spine structures include isolated ligament tests and bone-ligament-bone tests. Removal of the ligament from the spinal column for testing often damages the structure of the tissue and may lead to failures and big errors in the results. Bone-ligament-bone tests have the unique advantage that the ligament under test is not isolated from its surroundings. In general, to perform these tests at a specific vertebral level, all soft tissues are excised carefully leaving the ligament under test to be the only structure to carry the external axial tension [2].

In contrast to ligaments which are uniaxial (tension), intervertebral discs normally resist multidirectional loads. Discs carry compressive forces under all external loadings, except when direct uniaxial tension is applied. During normal physiologic conditions, the weight of the head compressed the intervertebral disc. Thus, the fundamental mechanical role of the discs is to respond to compressive loading. Like ligaments, the response of the disc depends highly on the magnitude and nature of loading. For example, under physiologic flexion (bending towards back) loading, as may be anticipated, the anterior disc carries compression while the load shared by the posterior annulus depends on magnitude of the flexion bending moment. In addition, because the head, which is approximately three times the weight of the neck, is not placed exactly on the cervical column, intervertebral discs do not carry pure compression [2].

In this study experiments were carried out on a bovine knee cartilage. The experimental data was used to obtain the material properties and the results were implemented to a finite element model of human cervical spine. In this model, the material properties of the disc were the material properties obtained from the experiment. The results of the finite

element analysis included the displacements and stress contour plot of the model under the applied boundary conditions. Comparing these results to the results reported in the literature, the validity of using animal cartilage for intervertebral disc was proven.

The method used in this study is an improvement to the approaches outlined in the literature study. This method was chosen based upon need for more comprehensive experimental data.

The next chapter is about the anatomy of human cervical spine and more specifically the anatomy of vertebrae and intervertebral discs will be introduced.

In chapter 3 some publications about the subjects of this study is introduced and their method and results are explained.

In chapter 4, the method of the experiment is explained. The source of material and method of preparation for the experiment and test protocol is described. The steps are all based on tested and proven methods performed by most researchers. The results of the experimental study are also shown in this chapter.

Chapter 5 is about FE analysis of the C3-disc-C4 section of the human cervical spine. The method of generating the model and mesh is described. The developed FE model consists of C3, C4, intervertebral disc and the ligaments connecting the two vertebrae. The material properties of the disc are what were obtained from the experiment and material properties of ligaments and bones are from the data reported in the literature. Then the results are compared to an experimental study on the same spinal section to validate the method of the experiment and the FE analysis. The objective of this chapter was to see if the FEM gives a good prediction of spine behavior under certain loads. If

the results obtained are satisfactory, then the accuracy of the results of the experiments and the validity of the test protocol are proven.

As a result, the test protocol explained in the experimental part of this study can be an improvement to what has been done so far by other researchers and can be the basis to design more complicated test protocols to investigate more material properties of cartilage. In addition, the FE analysis performed in this study, which was validated against the experimental works performed by other researchers, not only validates the results obtained from the experiment, but also proves the reliability of using FEM in analyzing the cervical spine.

2 The Anatomy of Cartilage and the Spine

2.1 Cartilage

The cartilage is an elastic, fibrous tissue located on the ends of bones. It allows the joints have smooth movements. It converts into bony structure throughout growth and development of body. The rest of the cartilage, which is not used for bone formation, builds the ears, nose, and joint cavities. It is a connective tissue that is important for its shock absorption properties [3].

Several painful joint disorders often take place because of the lack or degradation of this tissue. Based on its strength, elasticity, and structure, there are three different types of cartilage which will be discussed in this chapter [3].

The cartilage consists of cells, fibers and a matrix. After the birth and during the development, a dense connective tissue called the perichondrium encloses the cartilage. In adults, the cartilage of the ribs keeps its perichondrium, but that of the joints does not [4].

The only cells found in cartilage are Chondrocytes and their precursor, known as chondroblasts. Chondrocytes keep the matrix functioning and healthy [4].

As mentioned before, there are three different types of cartilage. The characteristics of each type are related to their purpose.

2.1.1 Hyaline cartilage

Hyaline cartilage is used more than the other types. This name is derived from the Greek word hyalos [4], which means glass and refers to the clear matrix or ground substance. Hyaline cartilage is normally the coating of the bones (articular cartilage). During the bone growth it is found inside as the center of the growth. Hyaline cartilage, also, forms most of the skeleton of the baby after the birth [4].

2.1.2 Elastic cartilage

Elastic cartilage and hyaline cartilage are so similar to each other but the elastic cartilage contains extended elastic bundles in matrix which causes a stiff elastic property for the cartilage. Elastic cartilage forms the ear and several tubes in the human body such as the walls of the auditory tubes. The important role of the cartilage is to keep the tubes permanently open [4].

2.1.3 Fibrocartilage

Fibrocartilage is a type of cartilage that provides stiff support in the areas that high tensile strength is required, such as between intervertebral discs, and at locations between tendons or ligaments and bones. The difference between fibrocartilage and the hyaline cartilage or connective tissue in that vicinity is not clear. The main difference between

hyaline and intervertebral disc is the collagen content [4].

Several studies have been carried out on the cartilage by employing a monophasic elastic model [5]. But the actual structure of the cartilage has two phases. The material of articular cartilage and meniscal tissue are similar. They are porous permeable composites composed of an organic solid matrix which are saturated with water. The water makes up 65–80% of the total weight of a normal tissue. The collagen fibres are the main structural components of the solid matrix that carry the loads. In articular cartilage, collagen makes up approximately 75% of the dry tissue weight [6].

The collagen molecules in both articular cartilage and menisci build the collagen fibres. However, the fibrillar structure of articular cartilage is normally smaller in scale than the fibers of the menisci. In addition, the articular cartilage and menisci are different in fiber distribution and orientation. On the surfaces of articular cartilage, the fibers are tightly packed and directed in a plane parallel to the surface of the bone. In the middle region, the fibers oriented randomly, while in the deep regions near the bone, the fibers are inclined to the direction perpendicular to the bony border. Unlike the articular cartilage, the main fiber direction of the menisci is circumferential, parallel to the edge of the meniscus [6].

The mechanical properties of the articular cartilage are distributed inhomogeneously. The mechanical material properties reported by Fithian et al. [6] are shown in Table 2. 1.

These stiffness values are similar or even lower than the reported joint pressures the materials have to carry which is 20MPa [6].

Table 1 Intrinsic moduli.

	Tension (MPa)		Compression (MPa)	Shear (MPa)	Permeability (m^4/Ns)
	Parallel*	Perpendicular*			
Cartilage	10.2 (s) 3.2 (m) 0.87 (d)	3.24 (s) 1.01 (m) 0.32 (d)	0.79	0.68	4.7×10^{-15}
Meniscus	198.4	2.8	0.42	0.112	0.81×10^{-15}

s = surface; m = middle; d = deep.
*Parallel and perpendicular to dominant fibre direction.

Table 2. 1 Mechanical material properties of cartilage [6]

Notable from this table is that the meniscal material is much stiffer in the circumferential direction compared to a direction perpendicular to the edge. Similarly, meniscal material is stiffer than the outer layers of cartilage. The outer surfaces of the cartilage are also stiffer than the middle and deep regions of cartilage [6]. The stiffness of the meniscus is half the stiffness of the cartilage in compression and only a sixth of cartilage in shear. These characteristics make the meniscus highly deformable and for this reason the meniscus can match complex geometries in different movements [6].

2.2 Vertebra

2.2.1 General structure

Vertebrae (singular: vertebra) are the uneven bones that form the vertebral column (spine), which is a flexible column. There are thirty-three (33) vertebrae in a normal human body. Five vertebrae are compound to form the sacrum . The rest of the vertebrae are separated by intervertebral discs. The upper three regions consist of the remaining 24 vertebrae. The spinal column has three regions: cervical (7 vertebrae), thoracic (12 vertebrae) and lumbar (5 vertebrae). The last number may be increased by an extra vertebra in one part. But the number of cervical vertebrae is rarely increased or reduced

[7].

A typical vertebra has essential parts: an anterior (front) segment, which is the vertebral body and a posterior part (the vertebral arch). This part encloses the vertebral foramen. The vertebral arch is formed by a pair of pedicles and a pair of laminae, and supports seven processes, four articular,

two transverse, and one spinous [7].

When the vertebrae are articulated with each other, the bones make up a strong column to carry the load of the head. They also create the vertebral foramina which constitute a tube to protect the spinal cord. There are two apertures, one on either side, for the spinal nerves and vessels [7].

Two transverse processes and one spinous process stand behind the vertebral body. The spinous process comes out the back; one transverse process lies on the left side, and one on the right side. The spinous processes can be felt beneath the skin in the cervical and lumbar regions. The role of the superior and inferior articular facets on each vertebra is to restrict the range of possible movement [7].

2.2.2 Cervical vertebrae

They are usually small and delicate [7]. Their spinous processes are short and sparated with the exception of C2 (2^{nd} vertebra) and C7 (7^{th} vertebra), which have spinous processes. Numbered top to bottom, atlas (C1) and axis (C2) are the vertebrae responsible for rotation of neck and head. The atlas allows the head to move up and down, but the axis allows the upper neck to rotate to left and right. The first intervertebral disc of spinal column is attached to the axis. The base plates and upper plates of the cervical vertebrae

are small and rectangular, the vertebral foramen has a large, triangular shape and the spinous processes are located horizontally [7] (see Figure 2. 1).

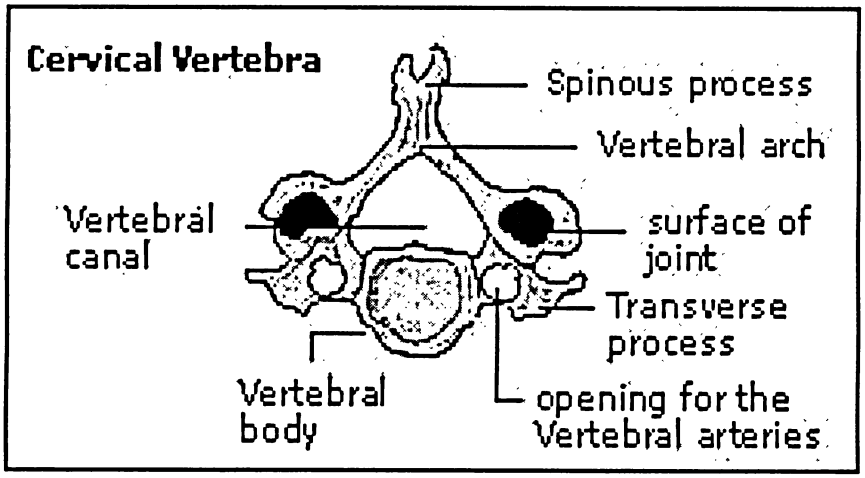

Figure 2. 1 Cervical vertebra [8]

2.2.3 Thoracic vertebrae

Their spinous processes have surfaces in contact with the ribs. Unlike cervical vertebrae, the base plates and upper plates of the thoracic vertebrae are triangular, the vertebral foramen has a round shape and the spinous processes point sharply downward [7] (see Figure 2. 2).

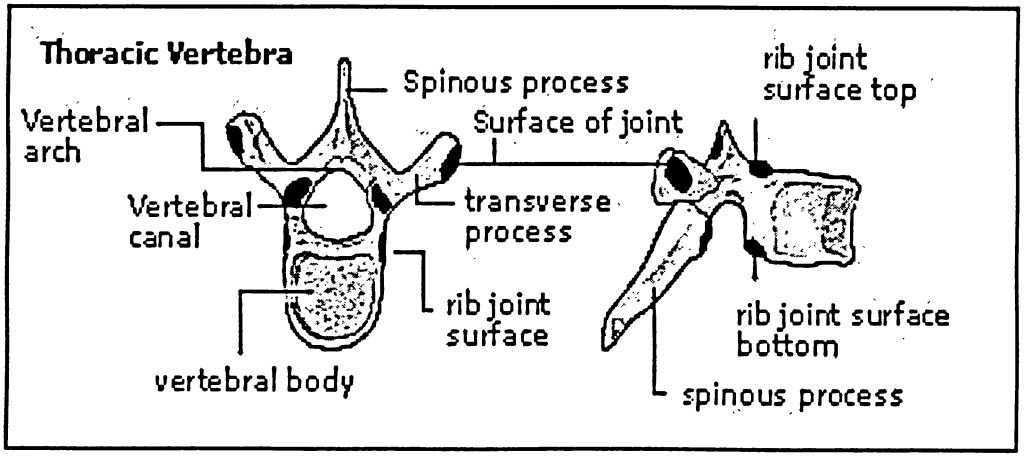

Figure 2. 2 Thoracic vertebrae [8]

2.2.4 Lumbar vertebrae

The structure of these vertebrae is stiff because they must support more weight than other vertebrae [7]. The discs between these vertebrae create a lumbar curvature that is concave toward the front in the human. The base plates and upper plates of the lumbar vertebrae are large and bean-shaped, the vertebral foramen has a small, triangular shape and the spinous processes are located horizontally. The fourth and fifth lumbar vertebra, carries the major part of the weight and the pain mostly takes place at this point [8] (see Figure 2. 3).

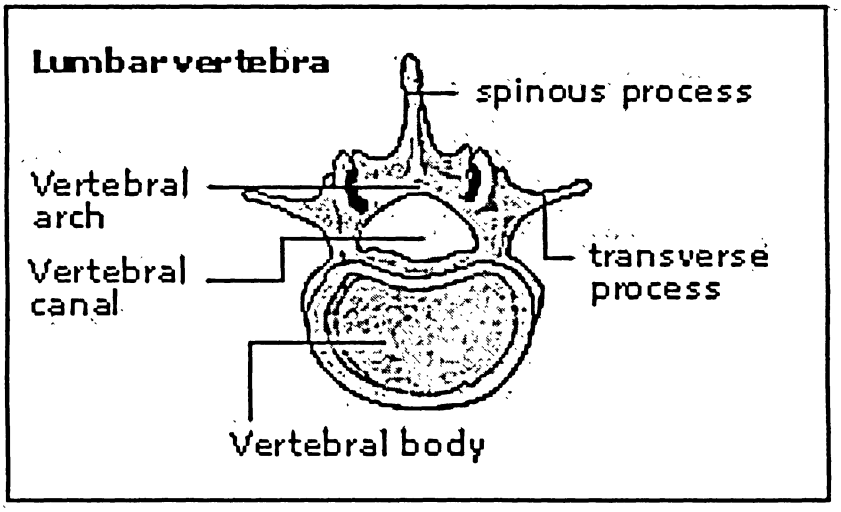

Figure 2. 3 Lumber vertebra [8]

2.2.5 Sacral vertebrae

There are 5 vertebrae which are called S1-S5 without any intervertebral disc in between [7].

2.2.6 Coccygeal vertebrae

This region has 3-5 vertebrae as well and again there is no intervertebral disc [7].

There are different vertebral forms based on mobility or load bearing requirements. However, the cervical, thoracic and lumbar vertebrae have structures similar to all vertebral bodies [7].

2.3 Structure of a Vertebra

The body is a cancellous tissue, which is covered by a thin layer of compact bone. The bony part has many orifices, some of which are large so the vessles can pass through. The arch and processes standing behind the body are covered with the compact tissue [9].

Figure 2. 4 shows different components of a vertebra.

Body (corpus vertebra): Being the largest part of a vertebra, the body is almost cylindrical in shape. The upper and lower planes of the body are flattened and coarse. These surfaces provide proper sites for the intervertebral disc to get attached, and each have a rim around its circumference. In front, the body is convex. Its anterior surface has a few small orifices, for the nutrient vessels and on its posterior surface there is a single large irregular orifice so the veins can come out from the body of the vertebra [9].

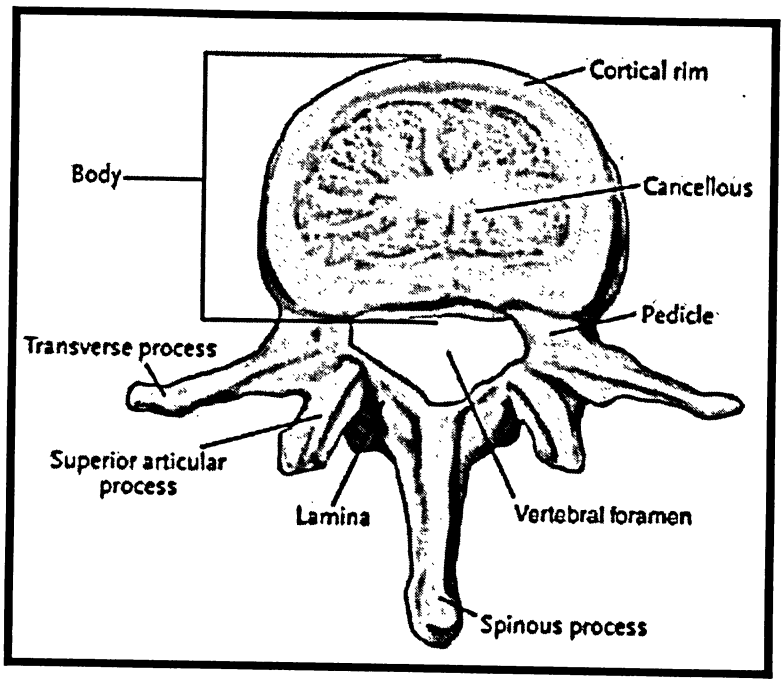

Figure 2. 4 Components of vertebra [10]

Pedicles (radices arci vertebræ): The pedicles are two short processes, which lie on the back side, on the upper part of the body [9]. The concavities above and below the pedicles are called the vertebral notches [9].

Laminæ: The laminæ are two large plates directed backward from the pedicles. They fuse in the middle line, and so complete the posterior boundary of the vertebral foramen. The upper borders and the lower parts of their anterior surfaces are rough for to attach the ligamenta flava [9].

Processes, Spinous Process: The spinous process is directed backward and downward from the intersection of the laminæ, and attaches the muscles and ligaments [9].

Articular Processes: The articular processes, which are two superior and two inferior, is seen at the intersections of the pedicles and laminæ [9].

Transverse Processes: The transverse processes, project one at either side from where the lamina joins the pedicle, between the superior and inferior articular processes. They attach the muscles and ligaments [9].

2.4 Vertebral Column

In human anatomy, the vertebral column (spine) is a column of vertebrae located in the back of the human body. It contains the spinal cord in its spinal canal [11].

2.4.1 Surfaces

Anterior surface

When viewed from front, the width of the bodies of the vertebrae increases from the second cervical to the first thoracic. There is then a slight decrease in the next three vertebrae. After that, there is again a gradual increase in width as low as the sacrovertebral angle. Right before the coccyx there is another sharp decrease [11].

Posterior surface

This surface of the vertebral column contains the spinous processes in the middle line. In the cervical part from 3 to 6 surfaces are short and horizontal. In the upper part of the thoracic region they are directed diagonally downward, in the middle they are almost vertical, and in the lower part and lumber region they are horizontal. There is the vertebral groove on both of the spinous processes formed by the laminae in the cervical and lumbar parts. These grooves contain the muscles of the back inside them [11].

Lateral surfaces

The articular processes in the cervical and lumbar parts separate the lateral surfaces from the posterior surfaces. They present the bodies of the vertebrae in the thoracic region by the facets to articulate with the heads of the ribs [11].

2.5 Intervertebral Discs

The intervertebral discs make up one fourth of the spinal column's length [8]. The intervertebral discs are found between the vertebral bodies combined with them. They have two major parts: an outer fibrous ring (annulus fibrosus) and a spongy center (nucleus pulposus) [12].

The intervertebral disc completely covers the lower and upper plate of each adjacent vertebral body. In the bony area, the outer part of the fibrous ring extends slightly beyond the circumference of the vertebral body to attach the disc more tightly to the vertebra [12].

About 80% of the spongy center (nucleus pulposus) of the intervertebral disc is water. The spongy center and the fibrous ring combine together to absorb pressures on the spinal column and transmit them to the adjacent vertebral bodies. The intervertebral discs function like a shock absorber, but most of the deformation is performed by the spongy center [12].

Different movements cause high compression and shear forces in the intervertebral discs. These forces must be damped by the intervertebral discs. Such loads applied upon the spine, force the fluid off the intervertebral disc and make it thinner. When the pressure is

relaxed, the disc sucks the fluid in again and becomes thicker. For this reason a person's height can vary by 1-2 cm during daytime activities depending on loads applied on the spine during the day [12]. This phenomenon is called 'Diurnal Change' and happens only in non-degenerated and healthy discs [13].

The intervertebral discs contain blood vessels until the fourth year of life, but, after the fourth year they receive the nutrients by diffusion. The intervertebral discs are in direct contact with the bony plates of the adjacent vertebral bodies [12] (See Figure 2. 5).

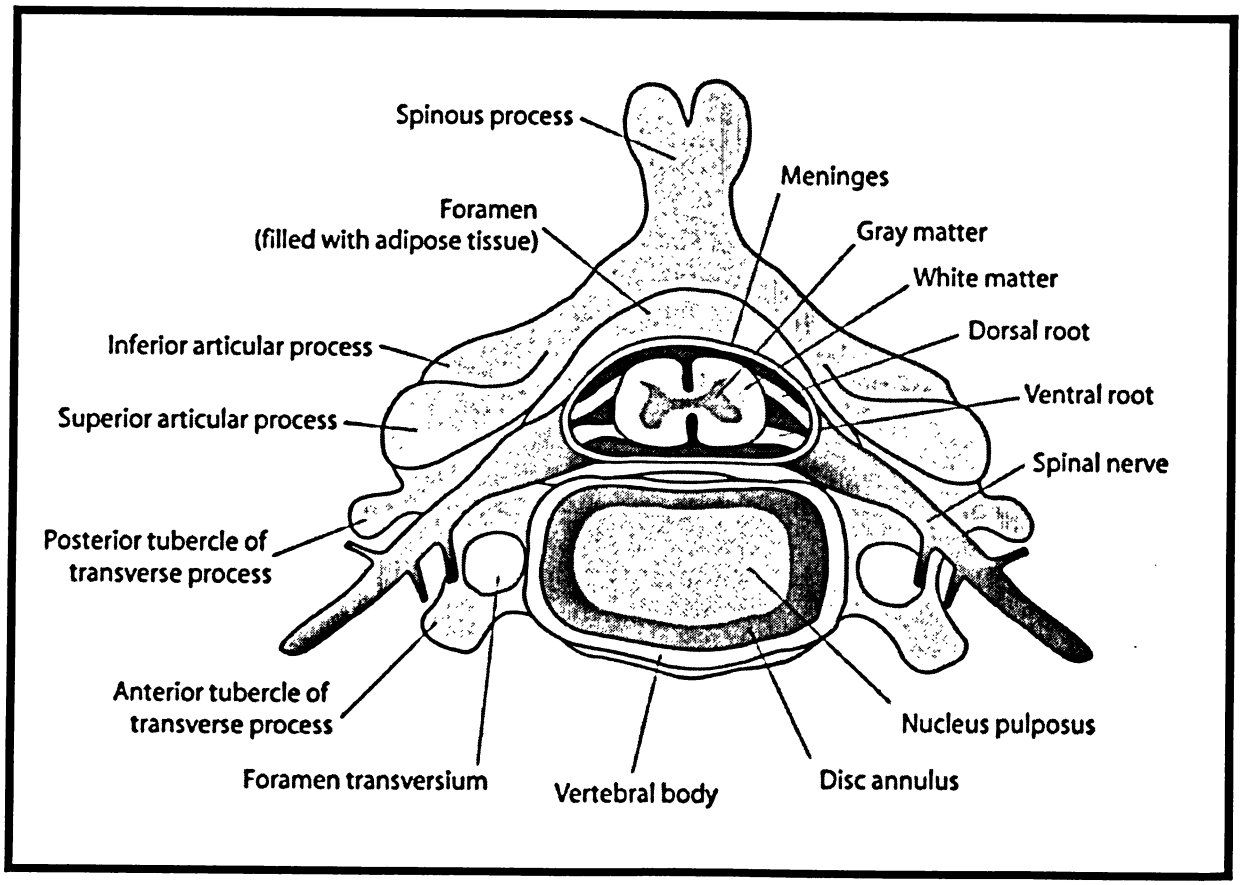

Figure 2. 5 The vertebra and the disc [12]

As the age goes up, they are not capable to take up water as much as before, which causes a drop in the swelling pressure of the spongy center. So the fibrous ring carries the pressures to which the vertebrae are exposed and therefore, at old ages the intervertebral

disc becomes less elastic and thinner. Then the base and upper plates of adjacent vertebrae become closer together. This results in the first bone-on-bone connection which forms osteophytes (new bony substance) on the upper or lower planes of the vertebral bodies which means that the intervertebral disc is degenerating [12].

2.6 Disc Function

In order for a disc (especially nucleus) to function well, it must have enough water content. A well hydrated disc is both strong and flexible. The nucleus pulposus needs to be strong and well hydrated to do its job (axial load), because it is this structure that carries the major part of the axial load of the body. With a healthy annulus, and a fully hydrated nucleus, the disc can easily support even the heaviest bodies! When the disc looses the water it loses capability to support the axial loads too, and this can cause a 'weight bearing shift' from the nucleus, outward, to the annulus and outer vertebral body [13]. This is 'over-load' on the annulus which may result in pathological DDD (Degenerative Disc Disease) [13].

Some tiny sponge-like molecules hold water within the disc. These 'super sponges' have an incredible ability to absorb and hold the water inside. They can hold more than 500 times their own weight in water. This gives the hydrated disc a high 'hydrostatic pressure' which is vital to bear the axial load and the body weight. This phenomenon which is called 'Diurnal Change' happens only in healthy discs. Disc cells, create, replace and rebuild molecules, and in order to function well it is so important for disc cells to have a non-acidic working environment [13].

2.7 Ligaments

Ligaments are fibrous tissues connecting two or more bones, cartilages, or structures together. They may be in the form of bands or sheets of connective tissues. The ligaments stabilize a joint during rest and movement. Harmful excessive movements such as hyper–extension or hyper–flexion may be restricted by ligaments. In addition, some ligaments do not allow the joints to move in certain directions [14].

There are three important ligaments in the spine which are the Ligamentum Flavum, Anterior Longitudinal Ligament and the Posterior Longitudinal Ligament (see Figure 2. 6) [14].

- The Ligamentum Flavum is a layer of tissue that connects the facet joints together to create a small cover over the posterior gaps between the vertebrae, and also protects the spinal cord [14].
- The Anterior Longitudinal Ligament attaches to the front of all vertebrae in the spine. This ligament is vertical (longitudinal) [14].
- The Posterior Longitudinal Ligament is vertically located behind (posterior) the spine and inside the spinal canal [14].

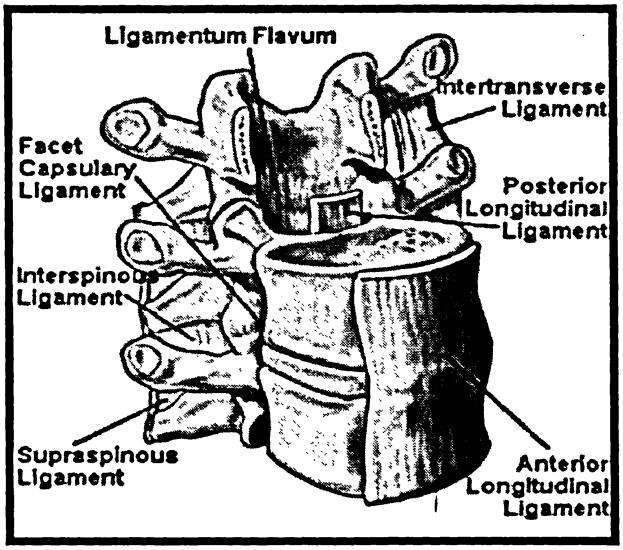

Figure 2. 6 Ligaments [14]

In Figure 2. 7 the vertebral column and its different regions are shown.

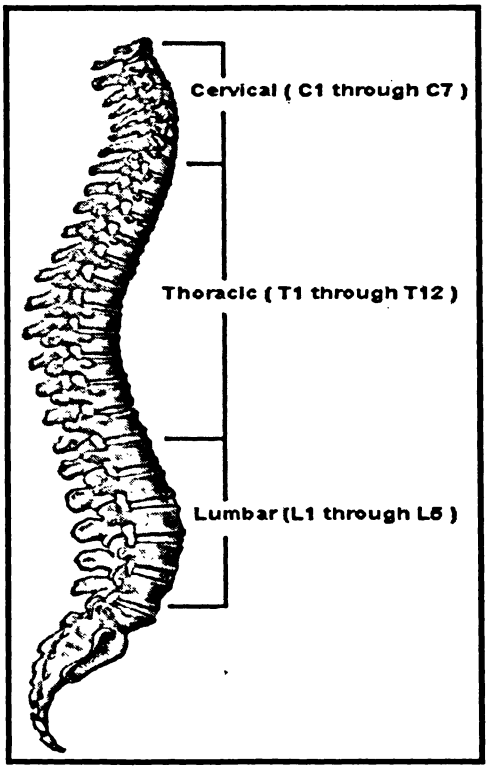

Figure 2. 7 vertebral column [14]

2.8 Coordinates and Terms

Medical professionals often use the anatomical planes to refer to a certain part of the body. These planes are imaginary lines passing through an standing body [15]. The terms used to describe each specific spinal plane are shown in Figure 2. 8.

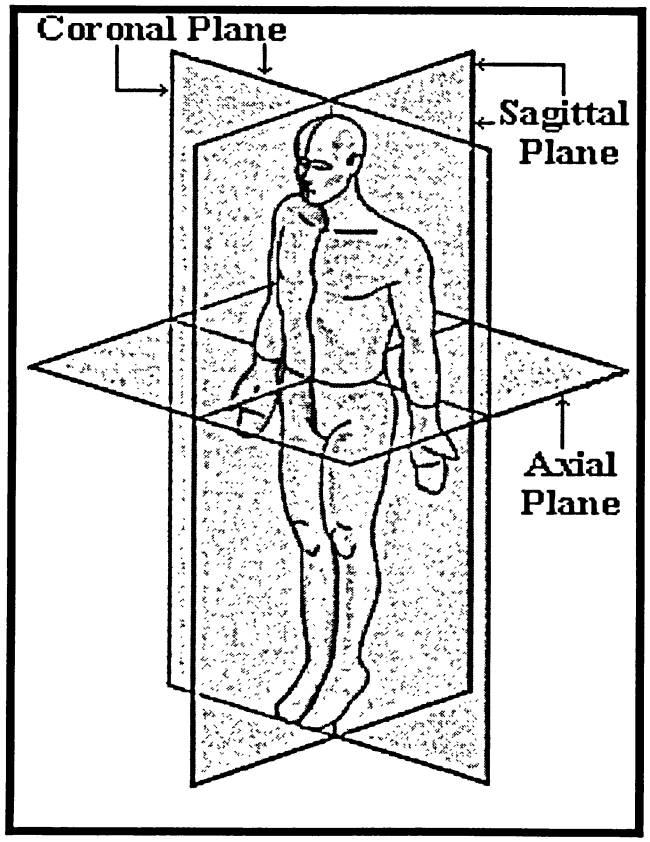

Figure 2. 8 Anatomical planes [15]

In the present study a three-dimensional coordinate system was defined for the model. The origin is located at the inferior-posterior wall of the body of the vertebra in the mid sagittal plane. The positive x-axis is directed to the left and perpendicular to the sagittal plane. The positive y-axis is directed upward, and the positive z axis is oriented anteriorly (See Figure 2. 9). The applied moments on the spine were defined as: flexion (+MX), left axial rotation (+MY) and right lateral bending (+MZ).

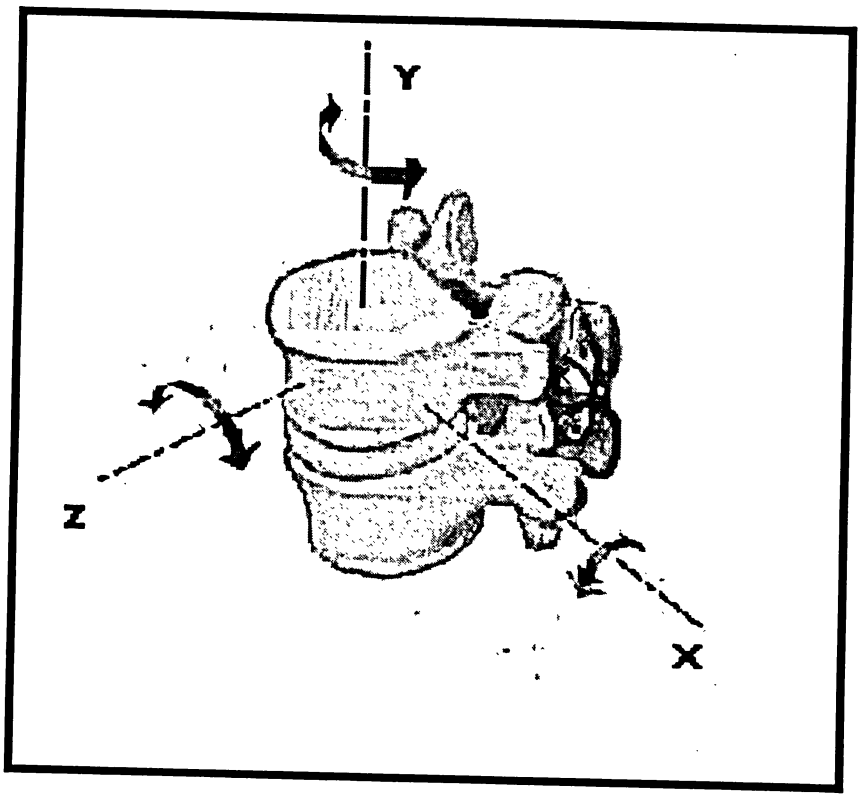

Figure 2. 9 Coordinate system

3 Previous Investigation on Cervical Spine

Testing the cartilage tissue in order to obtain the mechanical properties of this material has been one the most interesting subjects for biomechanical engineers since the birth of biomechanical engineering. The most important reason for the cartilage to be a vital tissue in term of mechanical performance is the fact that its role in human (or animal) body is sustaining mechanical load or absorbing it. Especially the cartilages in knee joints and intervertebral discs are usually under the weight load of the body above them, and that's why the fabrication of the artificial articular cartilage is another subject of so many publications. Among a lot of articles which have been published about the cartilage, most of them have tried to find a method to fabricate the artificial cartilage or repair the defective one. The study done by Yasuo Shikinami[16] is an example, in which an

artificial intervertebral disc was introduced that had improved properties compared with biological disc.

Abhijeet Joshi [17] assessed the compressive mechanical behavior of the PVA/PVP hydrogel nucleus implant as an artificial material for intervertebral disc. He tested this material in a confined compression test to prove that PVA/PVP hydrogels may be used as nucleus pulposus implants [17].

Hirokazu Mizuno [18] implanted intervertebral disc in mice. First samples were fabricated and then implanted in mice body. They were retrieved at several time intervals 16 weeks. At all intervals, samples had shape and it was seen that at some regions the tissue was formed. Histological and biomechanical analyses were carried out at each increment and the results proved the feasibility of implanting a composite tissue-engineering intervertebral disc with the properties of native tissue [18].

S.C. Fan et al. [19] worked on an analytical study to optimize the design of the intervertebral disc and analytically showed that the intrinsic design of the disc is the optimal structure. This can be a very helpful step in designing an artificial disc. In this study, they have carried out a stress and deformation analysis of the spinal disc, and proved that its deformations are invariant with the load intensity and only dependent on its dimensions and its constitutive property parameters. Thus, they demonstrated that the intrinsic design of the spinal disc makes it an optimal structure [19].

Peter Evans [20] designed intervertebral discs using computer aided tissue engineering based on the acquisition of vertebral CT scans of the lumbar spine. The artificial intervertebral disc was designed and analyzed in FE model using MIMICS software [20].

Lawrence M. Boyd [21] used mechanical requirements of functioning vertebrae as an objective to be achieved, and presented the steps of designing an intervertebral disc.

The second reason that articular cartilage and its mechanical characteristics have been the focus of much attention is that the most types of arthritis are associated with cartilage malfunction which usually happens when cartilage is damaged. It has been proven that mechanical loads can change the structure and shape of the cartilage which can result in the degeneration of the cartilage and articular diseases [22]. Therefore, studying the biomechanics of cartilage and its behavior under a combination of different loads is the first step to prevent arthritis.

Rani Roy et al. [23] carried out an experiment on cartilage taken from pig ears and ribs. The samples were stripes of cartilage and were tested in three-point bending apparatus. During the test the load and displacement were recorded which where used in large plate deflection theory to obtain the material properties of the cartilage. This theory was used because the length and width of the plate was much larger than its thickness. The error in their work was variable between 3.2% and 32%. Additionally, they investigated the variation of the stiffness of the cartilage after excision from the animal versus time [23].

M. Panjabi [24] studied the mechanism of whiplash, which usually leads to serious damages to the neck. In this study he calculated the dynamic vertebral loads throughout the cervical spine using inverse dynamics and calculated the dynamic intervertebral motions during simulated rear impacts of whole cervical spine model with muscle force reproduced and a substitute head. In this study he used six fresh-frozen human osteoligamentous whole cervical spine specimens, mounted on the testing machine as shown in Figure 3. 1 [24].

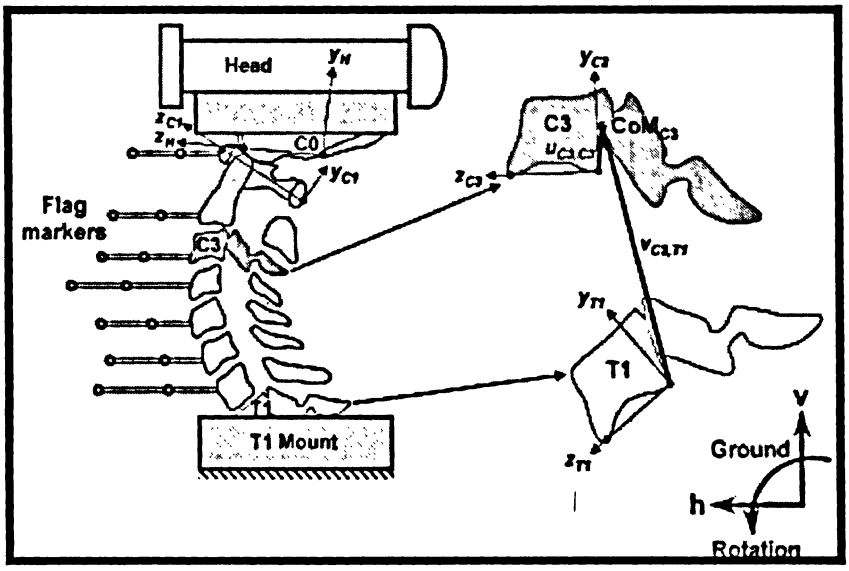

Figure 3. 1 A schematic of the whole cervical spine and anatomic coordinate [24]

The sample behavior was investigated based on the specific defined coordinate system and physiological properties of vertebrae [24].

In another study which was made by Panjabi [25], a similar approach is carried out but this time the experiment is focused on force replication for whiplash. The experiment is again on the six fresh-frozen spines (Figure 3. 2).

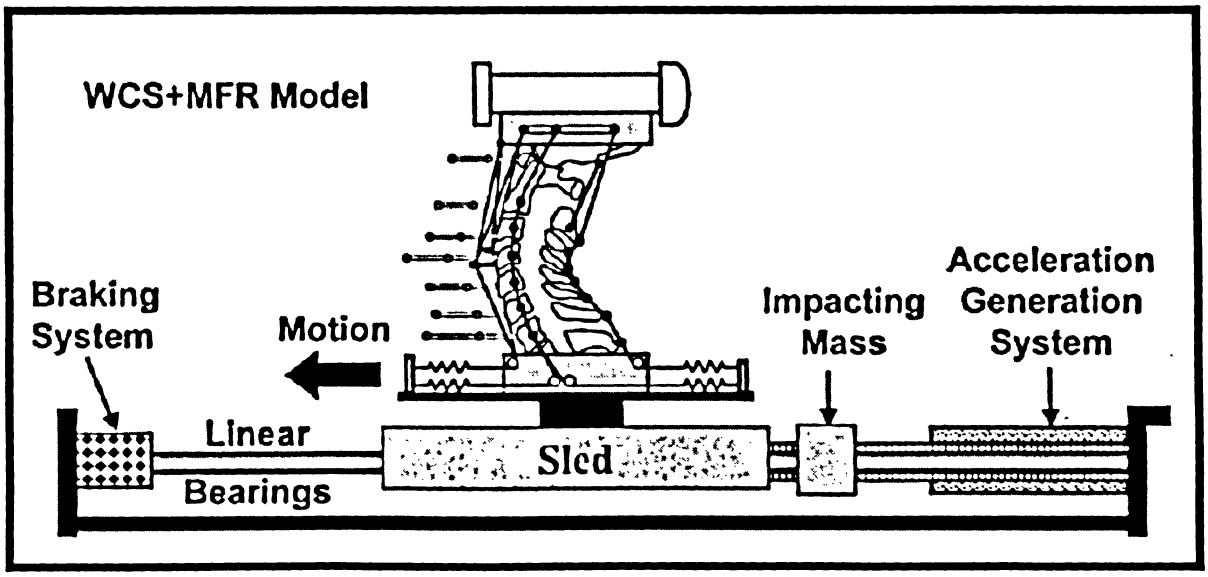

Figure 3. 2 Experiment apparatus [25]

Panjabi's [26] follow up study is about the effect of clinical spinal instability on lower back pain. A schematic load displacement curve of a spinal segment for flexion and extension motion is shown in Figure 3. 3. As seen, it is a nonlinear curve. The spine is flexible at low loads and stiffens with increasing load. The slope of the line (stiffness of the spine) varies with the load. This behavior is not adequately represented by a single stiffness value. They have suggested that at least two parameters be used: range of motion (ROM) and neutral zone (NZ). For the purpose of visualization, the load–displacement curve can be described by using an analogy: a ball in a bowl [26].

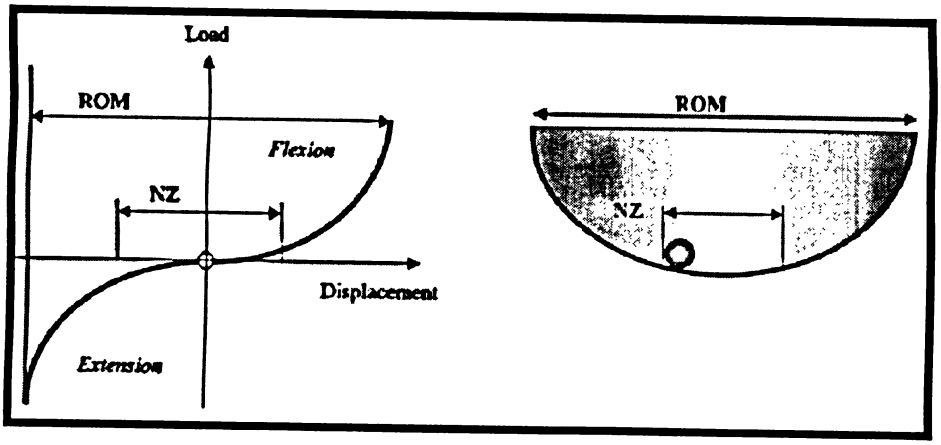

Figure 3. 3 Load displacement curve and ball in a bowl [26]

A deeper bowl, such as a wine glass, represents a more stable spine, while a shallower bowl, such as a soup plate, represents a less stable spine. He used this analogy in his research to describe the low back pain hypothesis [26].

In another experimental study, Panjabi [27] carried out an experiment about stability of the spine by means of an impact test on ten freshly frozen porcine lumbar spines. A functional spinal unit is a two-vertebra spinal unit with all the ligaments and the disc intact. 20 functional spinal units (FSU) were used. The specimens were wrapped in normal saline-soaked gauze and kept in sealed plastic bags at –20°C until tested. The specimen was damaged by releasing a mass through a guide tube onto an impounder on

top of the upper mount of the specimen. The motion of the impounder was along the linear bearings which were set in vertical direction [27] (Figure 3. 4).

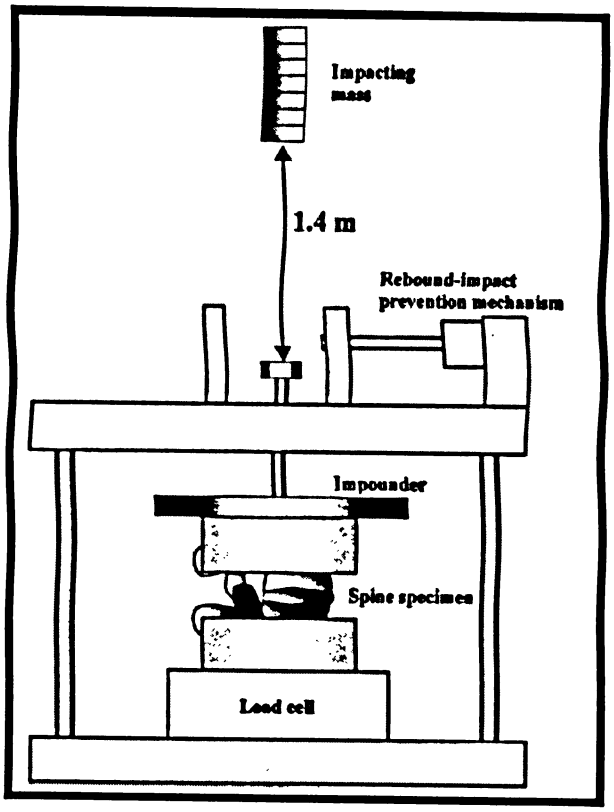

Figure 3. 4 Schematic representation of a specimen and the high speed [27]

After each traumatic impact, the specimen was resting for 1h to allow the ligamentous structures to recover [27].

Panjab et al. [28] worked on another experimental study in which the spine was compressed in an apparatus with increasing force until the point of buckling. The purpose of their study was to determine the critical load of the cervical spine in the frontal plane [28].

R. Gratz et al. [29] tried to measure the tensile modulus of the repaired tissue to examine the reliability of the planted cartilage. The samples were used in a uniaxial tensile test experiment and the data were used to calculate mechanical properties. Stress was simply defined as the load over the initial cross-sectional area of the sample in the centeral

region. The maximum load was the definition of the failure [28]. The stress following the relaxation phase at 20% elongation was calculated as an index of the overall tensile modulus of the sample [28]. They found out that there is no magnificent difference in modulus between repaired and intact cartilages.

Haisch et al. [30] studied the biomechanical characteristic of cartilage and their aim was very similar to that of Gratz [29]. They obtained human septal cartilage under sterile conditions from people who had corrective surgery. The samples were compressed between two pistons with a specific displacement and strain rate. A statistical analysis was performed afterwards to calculate Young's modulus and ultimate load/stress [30].

In order to assess the frictional properties of cartilage, which is one the most important properties of this tissue, Krishnan [31] studied the effect of dynamic loading on the frictional response of bovine articular cartilage. The objective of his project was to find out if cyclic loading and its frequency have any effect on the steady state friction properties of the cartilage and the interstitial fluid load support. In his experimental study, friction between bovine articular cartilage and glass were measured in unconfined compression under three dynamic loading frequencies representing physiological conditions (0.05, 0.5 and 1 Hz), and under a static load. His samples were obtained from bovine shoulder joints. The friction coefficient between cartilage and glass was measured in a phosphate buffered saline (PBS) bath, under the unconfined compression. They determined that the friction force is increasing with time, both for static and dynamic loading configurations and the friction coefficient under cyclical compressive loading oscillates above and below the response to static loading [31].

Chun-Yuh Huang [32] determined the tensile and compressive properties of human glenohumeral cartilage by testing 120 rectangular strips in uniaxial tension and 70 cylindrical plugs in confined compression, obtained from five human glenohumeral joints. The unique characteristic of his experiment was paying attention to orthogonality, that is, he cut the samples in two different ways: one in the direction of fibers and the other perpendicular to the fibers, and in this way he could capture anisotropic properties of the sample. Each tensile specimen was mounted in an Automated Tensile Apparatus and subjected to a tare load of 0.02N for 1000 s. In the tensile stress–relaxation test, the specimen was stretched using an increasing sequence of step strains and held for 20 min at each strain increment. During the test, the elongation and force were measured by a micrometer and a load cell respectively. The equilibrium tensile stress achieved was curve fitted by an exponential function to obtain the strain-dependent modulus of the sample. In the confined compression test, the specimen was mounted in the apparatus, and the tensile test was performed while the sample was in saline solution [32].

Oliver K. Erne [33] in 2004 worked on a similar project to investigate strain gradients in patellofemoral joint cross-sections of seven porcine specimens in response to 1% unconfined axial compression subsequent to specific amounts of off-set strain. He used an electronic speckle pattern interferometry (ESPI) system to investigate the strain distribution over the cartilage sample without contacting it. Delivering of high resolution and high-sensitivity strain contours over the cartilage cross-sections were the advantages of this method. The cubic samples were all obtained from procine knee joint and they were cut perpendicular to the surface of the cartilage. Specimens were gradually compressed to off-set strains of 5%; 10%, 15% and 20%. At each of these four off-set

strain levels, specimens were allowed to equilibrate for 1 h [33]. At each off-set strain level, specimens were incrementally compressed up to a total additional compression of 1%. Articular cartilage specimens showed depth-dependent strain distributions under uniaxial compression [33].

L.P. Li and W. Herzog [34] in 2004 published an article in which they showed the strain and strain-rate-dependent response of articular cartilage in unconfined compression. He showed for a given compressive strain, that the axial stress initially increases quickly, and then increases progressively more slowly towards the stress corresponding to the immediate response. Besides, they formulated fibrillar continuum element to replace the fibrillar spring element used previously in fibril-reinforced modeling, in order to solve the deformation incompatibility problem between the spring system and the nonfibrillar matrix. So their work has more focused on the effect of the strain-rate-dependent property of cartilage; moreover they have investigated the share of each part of cartilage structure (collagen fibrils and fluid) in carrying the load, in compression and tension. They compared the results obtained using the two fibrillar elements with the closed-form solutions for the static and instantaneous responses in large deformation case. So they found out that for unconfined compression, using the spring elements did not generally create greater numerical errors than using the fibrillar continuum elements [34].

Jahanessen et al. [35] published a paper in which they had determined the mechanical role of the nucleus pulposus in support of axial. The samples were obtained from sheep. Mechanical testing consisted of 20 cycles of compression–tension, a 1h creep, and a slow ramp test of compression. The findings of their study showed that functional evaluation of nucleus pulposus replacements and disc implants should include range of motion

(including neutral zone). For the test they made two bone-disc-bone motion segments per spine by making parallel cuts. After hydration and 18h before the test, the samples were stored in 4°C phosphate buffered saline solution. Then they were mounted on the designed apparatus for the confined compression test. The experiment was carried out in the room temperature and the sample was immersed in the saline solution during the test. The testing protocol is presented in Figure 3. 5. By 20 cycles they made sure that steady state was achieved, and it was obvious in the displacement diagram that it has occurred [35].

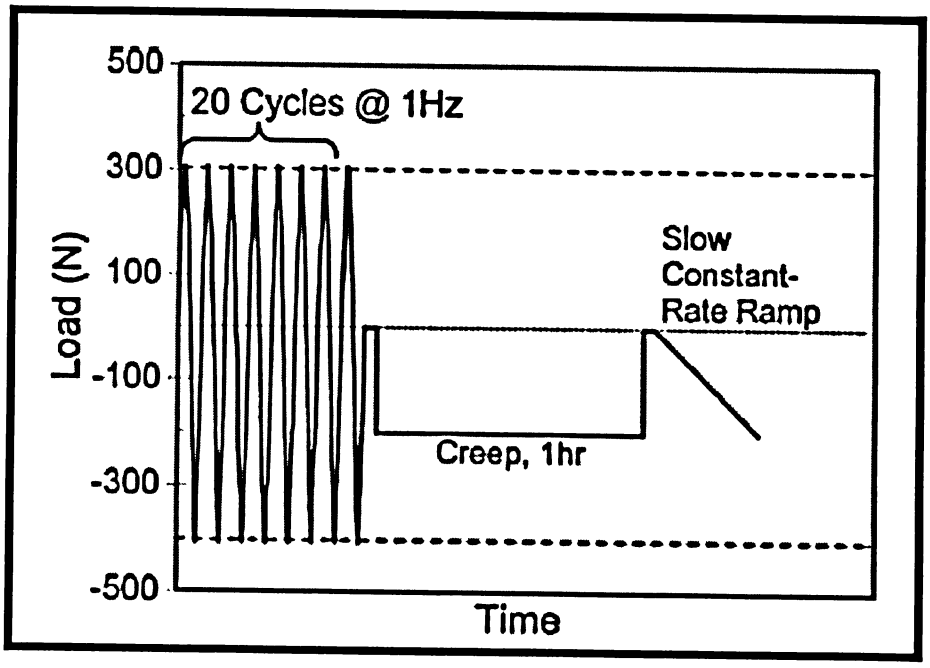

Figure 3. 5 The testing protocol [34]

James C. Iatridis et al. [36] had studied the intervertebral disc to obtain the effect of load and number of cycles of load on the damage of the intervertebral disc. They investigated the damage to the laminate structure of the annulus in the absence of biochemical activity in their study. The damage from the separation of annulus layers was examined. In this study, four rectangular tensile specimens oriented in the circumferential direction were excised from the outer annulus of 8 mature bovine discs that were approximately 4 years

of age and each of them was tested in one of four different tensile testing protocols. The effects of loading on the integrity and the composition of the specimens were investigated biochemically by measuring the total collagen content fraction of those fibers that were damaged. In this study, the discussion about the effects of the boundary conditions, number of cycles, the strength of load and the orientation of the sample on the damage of the sample is also interesting to note [36].

Daniel K. et al. [37] designed an in vitro biomechanical study using porcine lumbar motion segments to investigate the changes in the multi-planar bending properties of intervertebral joints following cyclic bending in different directions. He concluded that the change in mechanical properties of porcine intervertebral joints because of cyclic bending depends not only on the direction of loading but also the direction in which the properties are measured [37].

V. Yingling et al. [38] studied the dynamic loading on the characteristics of cartilage. They observed the failure mode versus the load rate for the samples obtained from pigs including three vertebral bodies and two connected intervertebral discs. They compressed the samples at five different loading rates to the point of failure. The results showed that the dynamic load increases the failure load of the samples as compared to quasi-static load but the rate of the dynamic load has no effect on the failure load. They plotted load-deformation curves to obtain a better understanding of the failure of the sample [38].

Jansen and DiAngelo [39] simulated the cervical spine by modeling it as a linkage system. The data used in their analysis was obtained from in vitro tests of fresh human cadaver spines. Their goal of was to determine appropriate rotational stiffness values by comparing the load vector with that of the experimental data. The cervical spine from C2

to T1 was modeled as a linkage system in which each vertebral body was a link. The geometry of vertebrae was approximated as a trapezoidal polygon. The dimensions were taken from anthropometric studies. The mechanical properties of the intervertebral discs were modeled as rotational springs with a linear stiffness, which means the torque acting in the spring was directly proportional to the rotation of the spring. Each spring in the model had the same stiffness value *k*. The rotational axis for each spring was located at the center of the vertebral body [39] (Figure 3. 6).

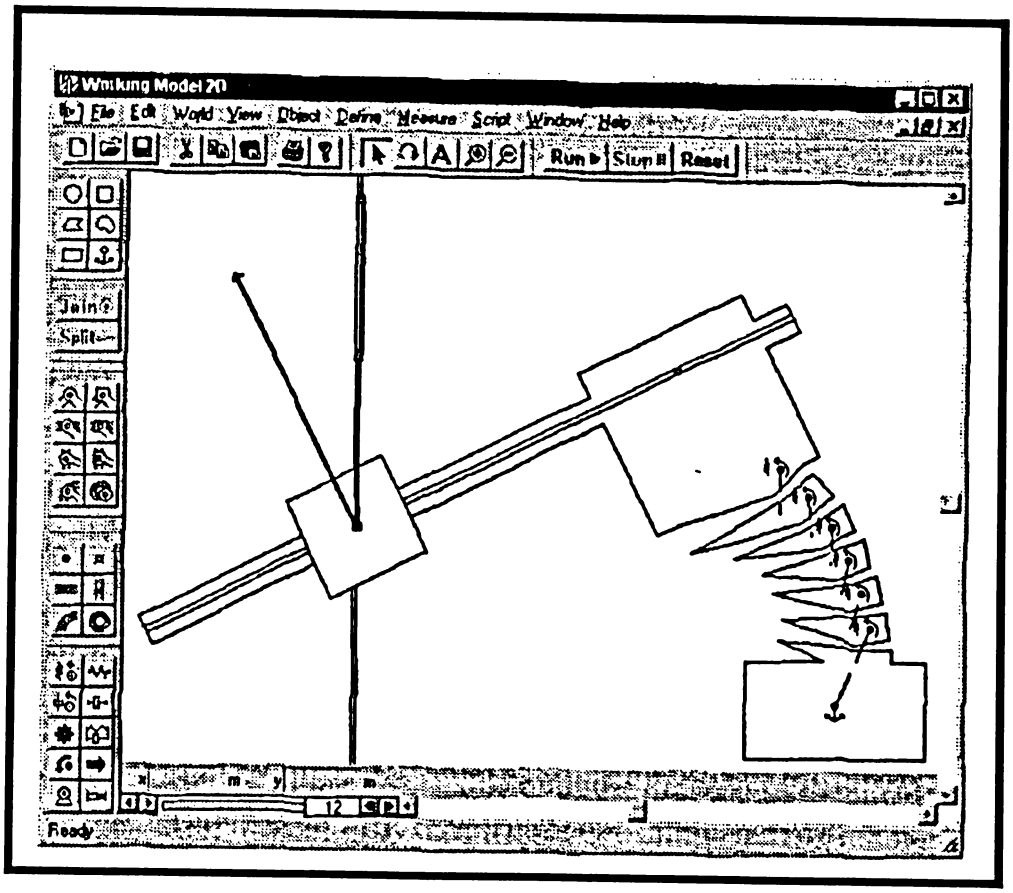

Figure 3. 6 Working Model simulation to verify the experiment [39]

T.S. Ching [40] carried out a study on the changes in the mechanical properties of inter-vertebral discs in vivo following static and cyclic compressive loadings of different frequencies. In this experiment, a rat-tail model of the intervertebral disc was used. Two sterilized gold-plated stainless steel pins were inserted percutaneously into the mid-

transverse plane of the 6th and 7th vertebral bodies by means of a specially designed alignment jig and a variable-speed electric drill [40]. Rats in the cyclic compression group were subject to a square wave compression between 7 and 15 N [40]. There were three loading groups to each of which a load frequency was designated [40].

The results in this study showed that changes in the inter-vertebral disc height depend on the frequency of loading. The decrease in disc height in the static compression group was greater than that of all other groups, whereas the decrease in the 1.5 Hz cyclic compression group was smaller than that of other compression groups. The mechanical response of the compressed disc depends on the applied stress and strain, but this study showed that the frequency of loading also has an effect due to the viscoelastic nature of the disc [40].

The test protocols in the experimental studies of the cartilage are usually very similar to each other and they have many points in common. However, there are some differences depending on the objective of the experiment and what the required data were. Since the studies were mostly regarding the mechanical properties of the tissue, the test in most cases included tensile or compressive test on the cartilage. Sometimes just the load-deformation curves were needed but sometimes the effect of loading was measured on another characteristic of the tissue (such as friction, degeneration, etc...). The tissues were usually obtained from human, pig or bovine, depending on the availability. Looking at the test protocols carried out so far, one can deduce or design a better test protocol that can produce a comprehensive data set.

In Roy's work [23], the samples were tested in an apparatus where load and displacement were measured during the test. Cartilage strips were mounted on the grips that were 5cm

apart and load applicators were located above the center of the sample. The thicknesses of the samples were measured by means of clipers. Data were sampled at 2 Hz rate and the rate of deflection was 0.00002 m/s. The samples were excised from pig ears and ribs. A Poisson's ratio of 0.4 was used for the model, although resultant E was insensitive to the change of Poisson's ratio [23]. (Figure 3. 7)

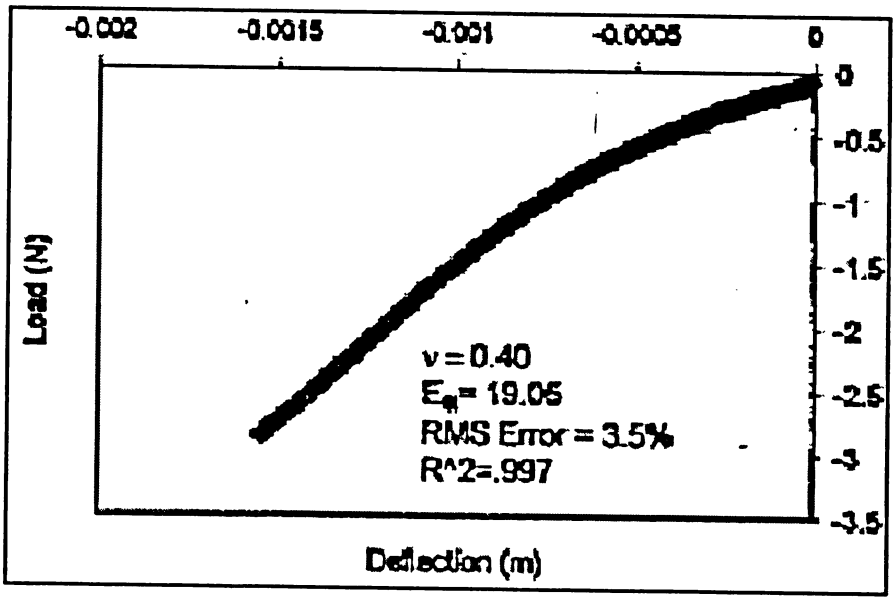

Figure 3. 7 Load deflection curve [23]

Their results showed that the articular cartilage has the Young modulus value of 15.56 MP.

R. Gratz et al. [41], performed tensile tests on a cartilage specimen. The thickness of the gage region was measured on each side of the center by means of a contact sensing micrometer. The sample was then clamped into a computer-controlled, uniaxial test instrument. The sample was run through a standard test cycle, while the load and displacement were measured. Sample hydration was performed throughout testing by continuous circulation of PBS. The sample was extended at 0.5mm/min until reaching a tare load, extended at a strain rate of a) 0.25%/s to the first 10% and then b) 20%

elongation (0.5mm and 1 mm, respectively) and allowed, at each position, to relax to for 900s, and finally, pulled to failure at a constant rate of 5 mm/min [41]. Failure, as defined in this study, happens when the stress reaches the maximum which is normally when the first tear is seen in the sample. Digital images of the sample were taken prior to testing, following the stress relaxations at 10 and 20% elongation, and at several points during the stretch to failure. Then the image processing was performed, which mostly focused on regions of interests (ROI) and the tear modes [41]. Correlation of each ROI was performed in the deformed images as shown in Figure 3. 8.

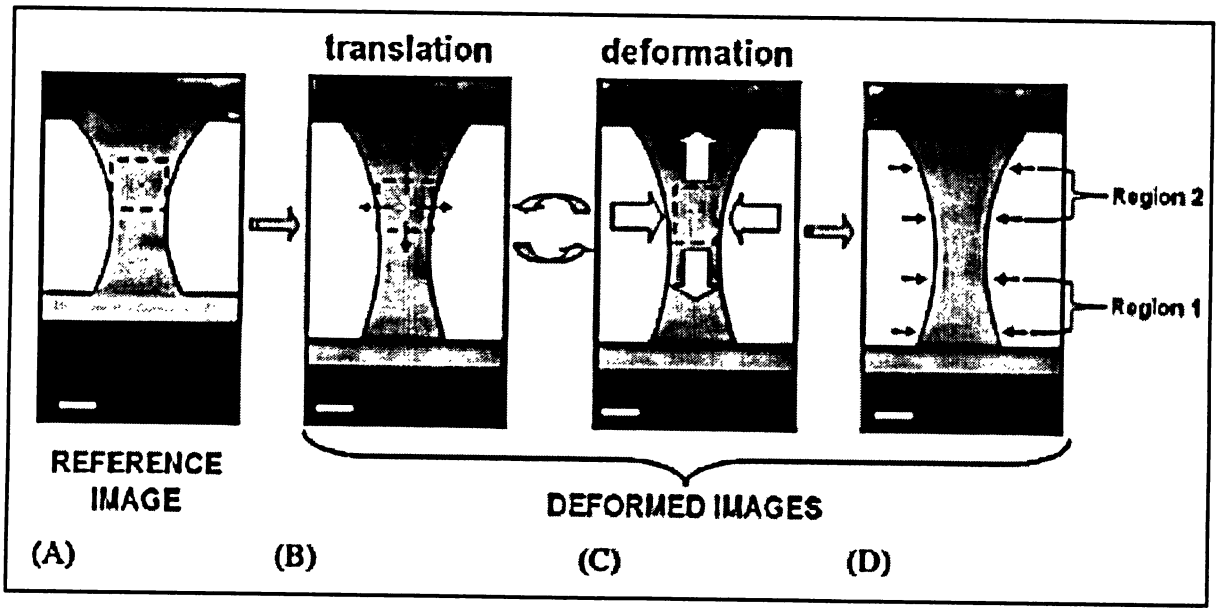

Figure 3. 8 The deformed images [41]

Then, the load and displacement data were used to calculate tensile properties. Stress was calculated based on the load over the initial cross-sectional area in the center of the gage region. Sample stretch was calculated as displacement over the distance between-clamp at tare load. The strength and elongation at failure were calculated at the point of maximum load. Equilibrium tensile modulus was calculated in different points by dividing the stress at 20% elongation by the strains determined from image processing.

Due to the fact that the width of the sample was variable along its length, the average stress was adopted which was 5–10% of the stress in the gage center. The data obtained from this test was used to investigate the tissue, recovered after in vivo cartilage defect repair, and calculate the tensile modulus of repair tissue [41].

O. K. Erne [33] used seven fresh frozen procine knee cartilages for the test. Cubic column specimens 5mmx5mmx7mm in size were excised perpendicular to the articular surface, using a diamond saw. All specimens had full-thickness cartilage and subchondral bone intact. Right before the test, specimens were thawed and to ensure proper surface properties to measure the stress. The subchondral bone of specimens was firmly fixed to a stationary grip which was a clamp. Both side of the articular cartilage specimen was unconfined. The sample was immersed in a physiologic saline solution during the experiment. Cartilage was compressed manually [33]. In Figure 3. 9 a: porcine specimen and b: experimental setup for unconfined compression is shown.

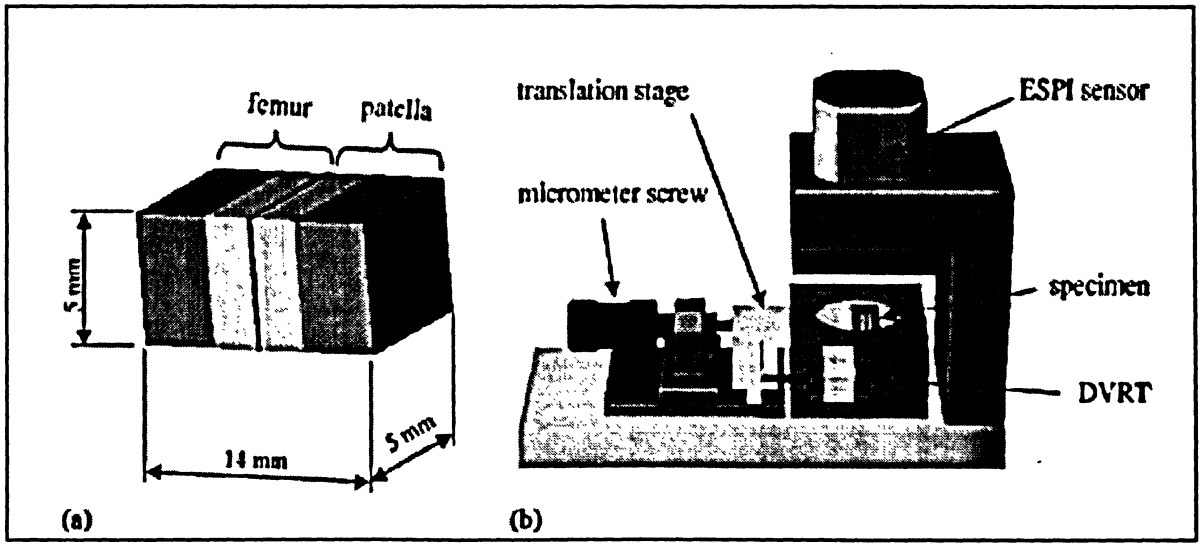

Figure 3. 9 a: porcine specimen, b: experimental setup for unconfined compression [33]

During the test, specimens were compressed to strains of 5%; 10%, 15% and 20%. Specimens equilibrated for 1 h, at all these four off-set strain levels. After equilibration,

were compressed incrementally up to a total extra compression of 1%: They used the results to prove that the strain distribution in articular cartilage is depth-dependent [33].

R. C. Evans [42] studied the relationships between solute diffusivities, mechanical properties, and matrix density of articular cartilage in compression. In order to carry out the experiment, the cartilage was excised from an 18-month old bovine humeral head. Then from each slice of cartilage, a 2mm disc was taken. Explants were stored frozen in PBS until the day of the test. Samples were bathed from one night before the test in a solution of fluorescent solute. For each solute, they used at least 15 cartilage samples from at least three different joints and then mounted the cartilage on the grips. They compressed and imaged the samples in a radially unconfined compression test. The samples were immersed in PBS all the time (Figure 3. 10) [42].

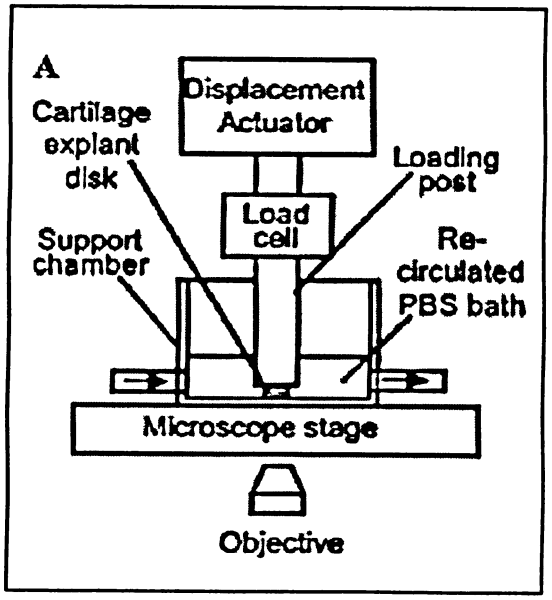

Figure 3. 10 Testing apparatus [42]

The compressive stress and cross-section geometry were measured during the test. The samples were then compressed up to 10 and 50%. Solute fluorescence intensity and

sample geometry were measured after mechanical equilibrium. The objective of this test was to measure the diffusion coefficients [42].

E. Tanaka [43] has designed a study to investigate the mechanical properties and load-relaxation of intervertebral discs in compression. He carried out the experiments on eight articular discs excised from eight adult dogs. First the muscles and other soft tissues were removed. Then the upper section of the joint was cut, and the condyle was excised along with the disc. Then, the disc was carefully separated. Right after removing the discs from the dogs, the experimental tests were performed, and the discs were immersed in 154 mM NaCl all the time. Figure 3. 11 shows the experimental system for the compression test. Compression was applied to samples up to the certain strain using a stepper motor. The forces were measured with a digital force gauge. A clip gauge with strain gauges was used to measure the distance between the two sides before and during compression [43].

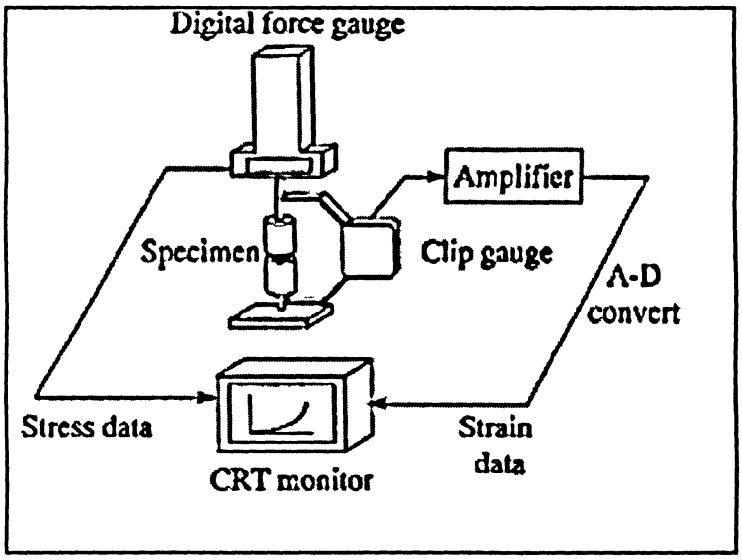

Figure 3. 11 The experimental system [43]

The samples were preconditioned before the load relaxation tests. Then the for load relaxation test, the sample was compressed from 0.25% strain to 2.0% strain at 0.25% strain intervals. The strain rate of this compression test was 20%/min and between each

increment the strain was kept constant for 2 minutes. To obtain the basic viscoelastic properties of the samples regression analysis was performed [43].

In order to investigate the effect of uniform heating on the biomechanical characteristics of the intervertebral disc in a porcine model, Jeffrey C. Wang [44] presented his method in testing the disc and tendon. The samples were porcine vertebra-nucleus pulposus-vertebra samples cut to a 1-cm diameter. He divided the disc core samples in two groups of five, and after bathing in 70C, tested at room temperature. Tendon and disc core specimens were subjected to mechanical loading on an MTS 632 servo hydraulic testing machine (Materials Test Systems, Minneapolis, MN) operating under stroke control [44]. Since the size of the disc core specimens was too small, the use of the extensometer for direct strain measurement was impossible. Therefore, displacement was recorded by the stroke indicator to measure the stretch. The strain of the sample was calculated as the elongation of the sample divided by its initial length. The slope of the stress versus strain curve obtained for the initial linear response region represented the stiffness of the specimen and the maximum load at failure represented the strength of the sample.

D. Spenciner et al. [45] designed a test protocol to study the multidirectional bending properties of the human lumbar intervertebral disc and determine the bending stiffness, range of motion (ROM), and neutral zone (NZ) of the human lumbar disc in multiple directions. They used human lumbar anterior column as samples. First they removed the posterior elements from functional spinal units. During the test the discs were kept bathed in 0.9% NaCl saline solution. Befor the test the samples were kept in bags in -20C until the day of the test. A six-channel load cell (model MC3-6-1000; AMTI, Watertown, MA)

acquired load and moment data about three orthogonal axes while linear and rotary motions about the vertical axis were measured with the load frame transducers [45].

H. C. Wu [46] carried out a study to determine the mechanical behavior of the annulus fibrosus. He tested human postmortem annulus fibrosus specimens in his experiment. Specimens were normal discs obtained from people between 20 to 30 years old. The samples were rectangular blocks cut from the intervertebral disc. He used a universal testing machine (Instron TM- 200) to test the specimens. The displacement rate was kept at 0.005 in/min. He used Eastman 910 adhesive to glue the specimen to the grips. Testing the specimen was started 3 minutes after the gluing the sample to the grips. In order to ensure the homogeneity of the deformation of the sample, two parallel lines were stamped on the surface of the specimen. The strain was measured by means of an optical method. A camera took the pictures at each increment for image processing. The longitudinal and were obtained by enlarging the pictures. Magnifying the pictures they obtained the transverse extension ratios [46].

FEM is the choice of most of researchers as the best mean to capture the best numeric results. H. Weinans et al. [47] discusses the effect of intervertebral disc characteristics on load distribution on the vertebral body. They developed a method to measure the tissue strength of trabecular bone from axial CT-scans obtained three dimensionally combined with a FE model. Their method obtains the stress distribution in the structure. It can be used to measure the strength and fracture risk of the bone. In their study they investigated the external loading conditions on the vertebral body, because it might be highly affected by the behavior of the intervertebral disk. The discs had both nucleus and an annulus region. The bone was a 3D model and the FE model was generated and the brick element

was used as shown in Figure 3. 12. In their model the elastic modulus of every element depended on the local density value: $E=2610p^3$, where E is the elastic modulus in MPa and p is the apparent bone density in g/cm^3.

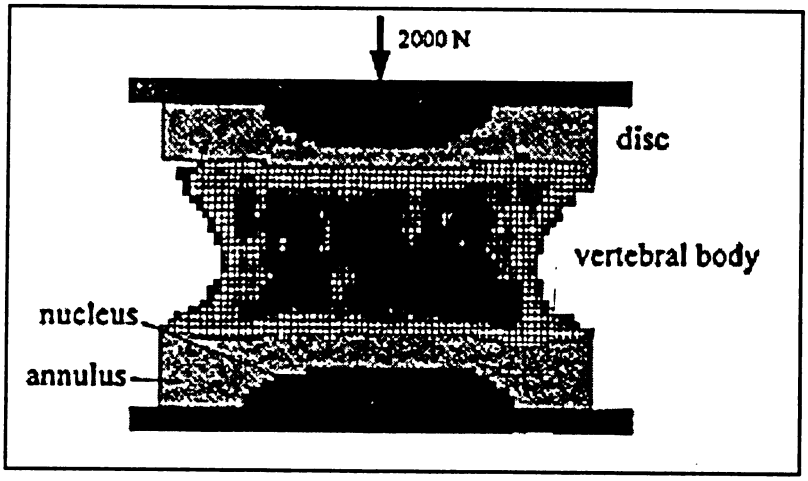

Figure 3. 12 Finite element model [47]

An artificial intervertebral disc was at the upper and lower endplate portions in the model. The brick element of the both discs had the same size. The intervertebral discs contained two types of material properties due to its nature, which consists of the nucleus pulpous and the annulus fibrosus. They were modeled as linear elastic materials. The Young's modulus of the annulus fibrosus was set at E=10 MPa and three moduli for the nucleus were implemented: E=l MPa, E=10 MPa and E=100 MPa to examine the sensitivity of the model to material properties. A 2000 N Force was applied. Their model consisted of 100,867 brick elements including all parts. The stress, strain, and strain energy distributions throughout the vertebral body were assessed. They showed that there is a relatively high loading on the vertebral body's cortical shell.

Luzhong Yin and Dawn M. Elliott [48] created a homogenized model of Annulus Fibrosus. Homogenization theory assumes that the material is composed of identical volume elements and based on this assumption explains the effect of microstructure on

macroscopic material properties. They compared model predictions to annulus fibrosus properties which was obtained experimentally and carried out a parametric study [48].

A. Shirazi-Ad1 and Harcharan Singh Ram [49] published a paper in 1995 in which they simulated a 3D finite element model of human intervertebral discs (Figure 3. 13) to examine the effect of change in the content of nucleus fluid on the general mechanics of a lumbar motion segment. In their model the disc annulus is a nonlinear, non homogeneous composite collagenous fiber which embedded in a matrix of ground substance and the disc nucleus is an inviscid fluid. The facet joint is modeled as a moving nonlinear frictionless contact problem, and uniaxial elements with nonlinear material properties are used to model the ligaments.

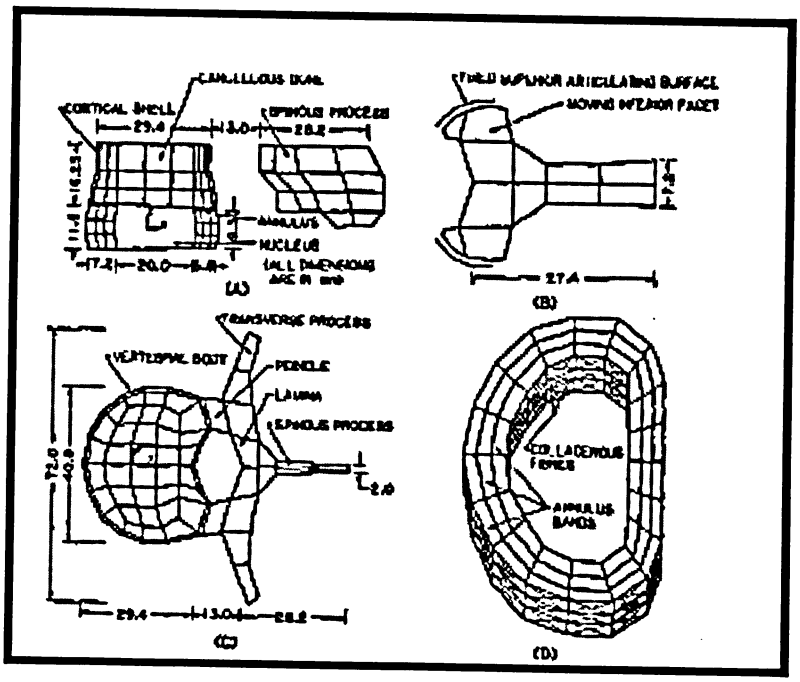

Figure 3. 13 FE model [49]

A three-dimensional nonlinear FEA of the interbertebral discs under complex loads has been done by Jun Yao et al. [50], in which they determined the optimal Young's modulus and the failure strength for the artificial scaffold under different loading conditions. They

examined the performance of the implanted scaffold and its effect on the mechanical behavior of the intervertebral disc. In order to model the disc and vertebral body, they made a few assumptions. First was the symmetricity of the anterior component of a disc unit (the intervertebral disc and adjacent vertebral bodies) which was modeled as a as a 3D structure. Second they neglected the loads transmitted outside the body of the vertebrae during small axial deformations. They did not include the anterior and posterior longitudinal ligaments. They assumed that two adjacent vertebrae and their intervertebral disc are symmetric about their horizontal center-planes. So, their model was divided into 6 distinct segments. They used the program ABAQUS to generate the FE model (Figure 3. 14). They used 3D eight-node brick elements to mesh the model while 3D hydrostatic fluid elements were used for the incompressible nucleus pulposus (incompressible fluid assumption).

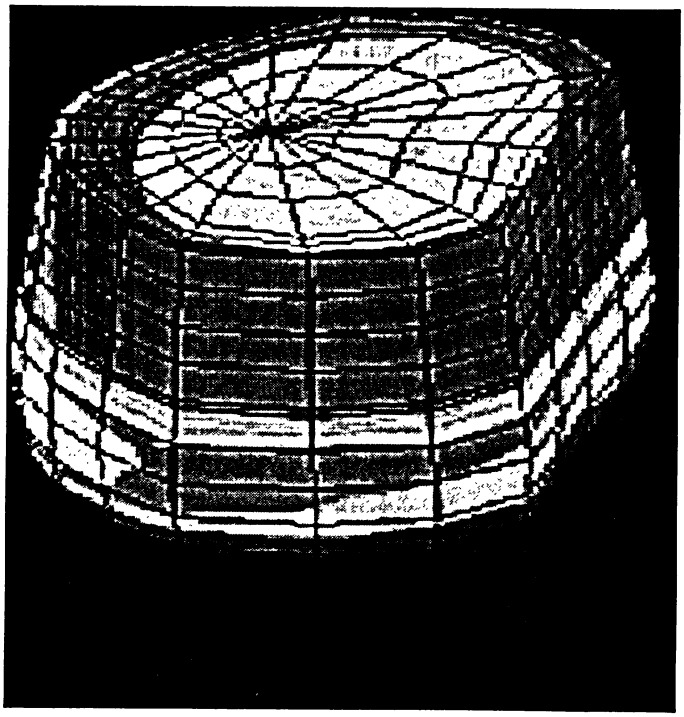

Figure 3. 14 FE model [50]

They simulated the model isotropic in all properties except in E, in which they assumed that the material has about 30% difference in z direction from two other directions. Bone, endplates and the ground substance were modeled linearly elastic. The segment C2–C3 was under the load of forces and moments, which were applied to the center of the mass of the C2 vertebra. The C3 vertebra was fixed in all directions. The load conditions in different simulations consisted of the axial compression, the shear stress, the torsional rotation in the sagittal plane and the lateral bending. The lumbar motion was under axial torque applying rotation moment to the C2 top surface. A lateral bending moment about the longitudinal axis was applied to the C2 top surface.

They found results obtained from this simulation satisfactory as compared to the published experimental results because no significant difference was found between the prediction of this model and experimental data.

Hung-Wen Wei [51] generated an FE model to investigate the effect of the mechanical properties of the subchondral plate, femoral head and neck on the stress distribution in the articular cartilage. They simulated FE model with dynamic loadings to study the effects of changes in mechanical property of the underlying bones of the proximal femur on the stress distribution in the cartilage of the hip joint. They generated a 2D FE model simulating the hip and supporting tissues for contact analyses using ABAQUS software. They performed a preliminary static analysis to verify this FE model. This FE model had 4974 four-node bilinear elements and 38 three-node bilinear elements. The loads of 600N as the bodyweight, 2000N as the abductor muscle force, and 100N as the adductor muscle force were applied at the joint [51] (Figure 3. 15).

PROPERTY OF
RYERSON UNIVERSITY LIBRARY

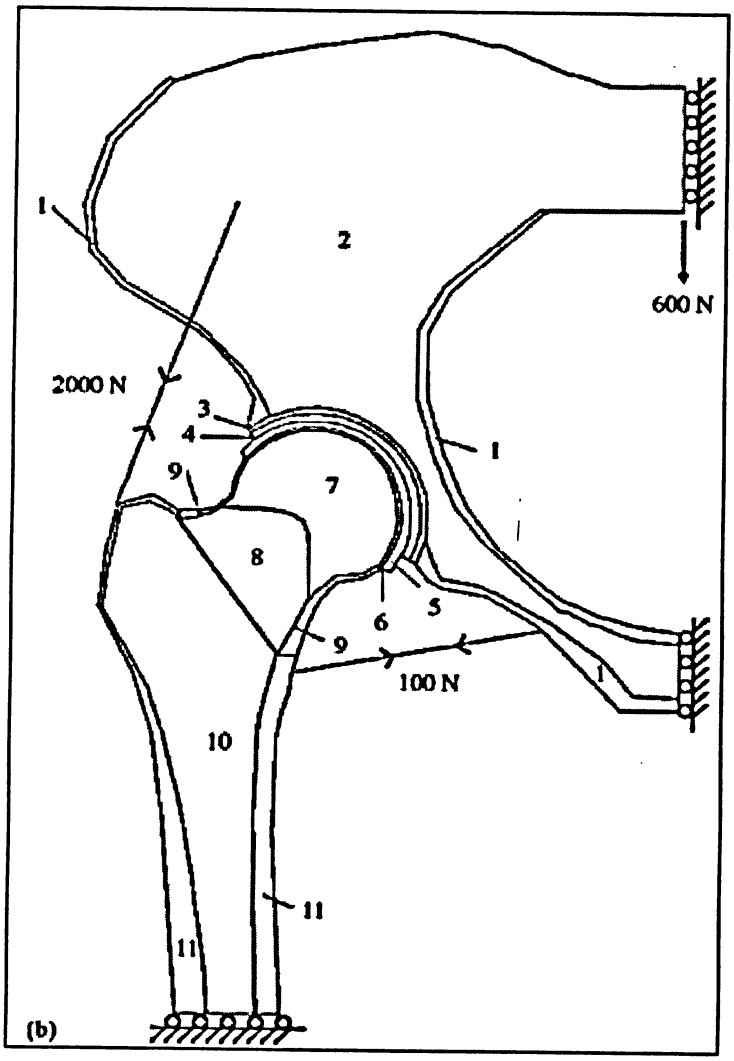

Figure 3. 15 Static model [51]

They assumed that the hip joint could carrye. They proved that the stress oscillation from impact is more harmful to the cartilage than the static loads as a result of a higher stress level. The published data about elastic modulus and the damping coefficient of human cartilage was used as the material properties of the cartilage in this study.

Despite the fact that many researches have been carried out to investigate the material properties of the cartilage and intervertebral disc, they mostly focused on the material properties obtained from a confined compression tests; also, in the majority of the experiments the cartilage was tested intact and few studies were related to the in-plane

testing of cartilage. In addition, few researches have been performed to model the intervertebral disc accurately in a finite element model. The models generated so far in the literature were all created by the authors and there is no FE simulation using an accurate geometry of this tissue. Designing a protocol to obtain the material properties of the cartilage via an in-plane tensile testing and using the results in an accurate FE model may be good improvement to the studies explained.

4 Materials and Method

As was mentioned in chapter 1, biological materials are, in general, a nonlinear, anisotropic and viscoelastic medium. Considering these characteristics into account, determining mechanical properties is extremely difficult if not impossible. In this study, the cartilage was assumed to be linear isotropic elastic with no viscoelastic response.

In this chapter the testing apparatus, test protocols, experimental data and material parameters are explained.

4.1 Testing Apparatus

The testing machine utilized here was designed so that in plane uniaxial, biaxial and pure shear test could be performed on membrane.

This testing unit is very versatile and can perform various testing protocols. The apparatus was primarily designed for soft tissue testing and it can also perform testing on elastomers and rubber like materials. Each axis of this biaxial machine is operated

independently so that any configuration of uniaxial as well as biaxial testing can be performed. Two load transducers are used, one for each axis, to read the applied load and record them to a data file through a data acquisition system. In the uniaxial and biaxial testing protocols, the grip can cause stress discontinuity near and around the grip section. Thus, it is essential to measure the displacement at the center of the specimen. To do this, A CCD camera was adapted to the system to measure the displacement at the center of the specimen.

Two stepper motors were utilized to apply the displacement to the test sample through lead screws. On each axis, one left-handed and one right-handed threaded rod were used. The two threaded rods were connected axially to each other so that when displacement is applied, the two cross head of the machine were pulled apart equally and the central region of the test specimen did not move away from the center. The outward motion of the pulling arms, oriented along two mutually perpendicular axes, pulled the edges of the specimen. The stepper motor controls the stretch (strain) applied to the test specimen by pulling cross heads apart. The cross head and the grip assemblies ride on linear bearings to provide a smooth motion to the displacement control test protocol.

Customized software was developed to apply the displacement and to simultaneously record the load, displacement and the corresponding image from the CCD camera to a data file. The apparatus is capable of applying uniaxial, biaxial and in-plane shear load to test specimen under various strain rates. Commercial software (EasyAccess) provided with the CCD camera was used to determine the deformation in the central region of specimen. Figure 4. 1 depicts the testing apparatus.

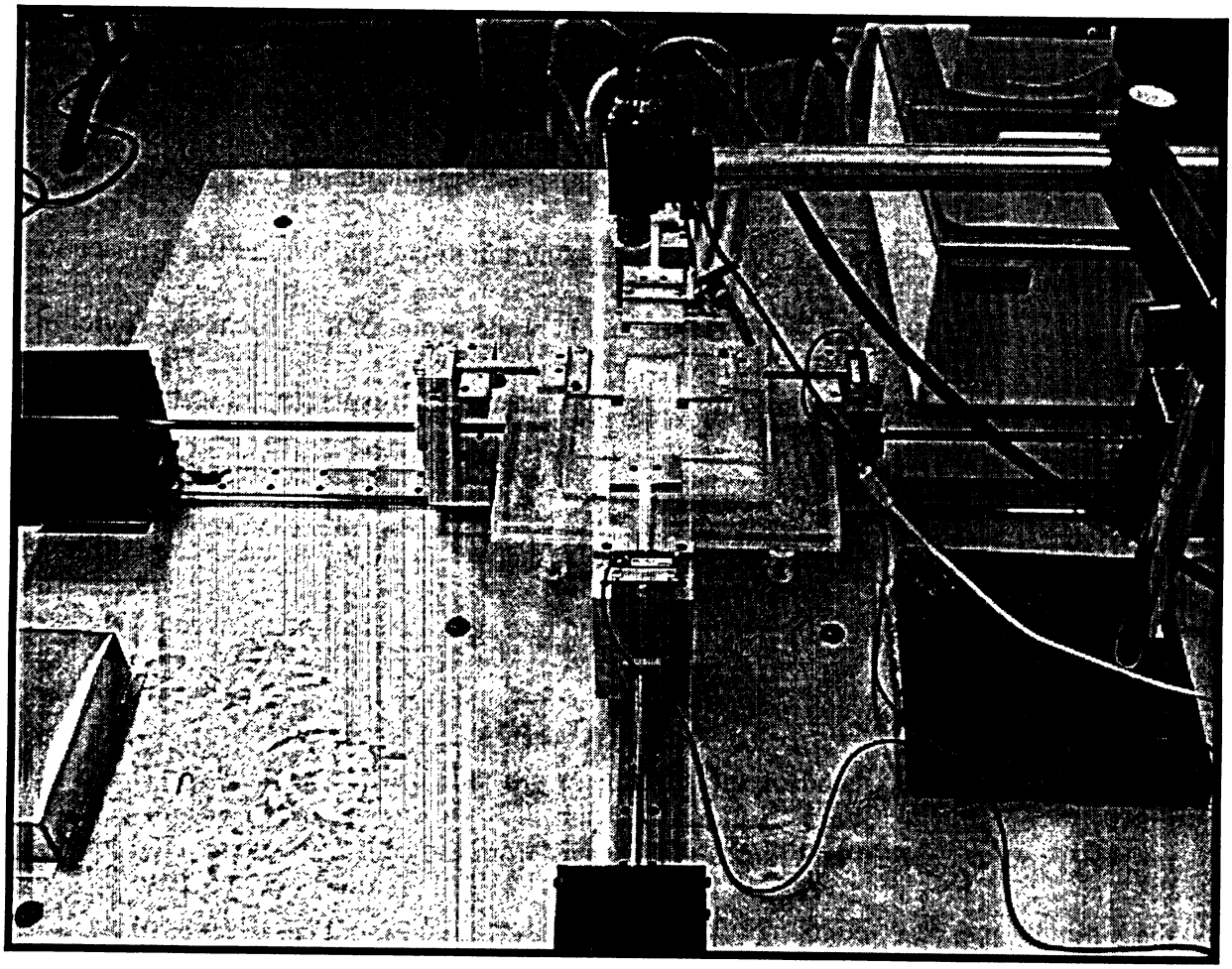

Figure 4. 1 The biaxial testing machine

4.2 Experimental Test Protocol

The cartilage used as a test specimen was obtained from the freshly frozen knee joint of a one to two-year old bovine. The knee joint was wrapped and sealed in the slaughter house just after slaughter. The sample was brought to the lab quickly and was frozen freshly until the day of the test. It has been assumed in many biomechanical engineering experiments that if the sample is frozen after the excision from the animal until the time of the test, the mechanical properties of the tissue will remain unchanged [31, 32, 33, 44, 45, 35, 18, 52, 53, 54]. In this experiment, because no dissection is done and the tissues were frozen in their natural state, the anatomic integrity of the various hard and soft tissue

structures and their relative position were not compromised [53]. At the day of the test it was brought to the lab and left for 3 hours to be defrosted. The tendons and the connective tissues were cut and removed very carefully so that no damage to the cartilage occurred. After cutting the connective tissues, the two parts of the joint were separated. After the whole part was defrosted, the cartilage on the surface of the bone was ready to be cut off. A surgical knife was used to cut the cartilage sample from the surface of the bone. This was done very delicately to ensure that the sample has uniform thickness.

After the initial sample was cut from the bone, the rectangular sample was cut by means of a surgical knife. A small square is marked at the center of the sample for image processing using enamel ink. At this point the sample was ready to be mounted on the testing machine. Before the sample was tested, the thickness was measured by optical micrometer for future data analysis.

In order to maintain the properties of the sample and to hydrate it during the test, Phosphate Buffer Saline (PBS) solution was used. This solution is a popular saline solution employed in many biomechanics engineering experiments [30, 32, 32, 56, 57, 43, and 53]. It is a salty solution containing sodium chloride, sodium phosphate and potassium phosphate. The buffer helps to maintain a constant pH. The concentration usually matches the human body (see Table 4. 1). When the sample is mounted onto the grips, the saline solution is being circulated through the circulating apparatus to the saline solution bath in which the sample in fully submerged. The circulating machine is Neslab EX 10 (Thermo, ELECTRON Corporation). The solution is transparent and has no color so it does not influence the focus of the image taken from the CCD camera.

NaCl	7.650 g
Na_2HPO_4, anhydrous	0.724 g
KH_2PO_4	0.210 g
Distilled water	1 liter

Table 4. 1 PBS solution components [57]

For this experiment, a set of grips were designed. This grip comprises of a 0.125" diameter rod with six equally spaced holes and six straight wires with 0.0375" diameter of equal length. One end of these wire are bent into a U-shape while the other end of the wires are passed through the holes of the 0.125" diameter rod and twisted to form a solid connection. For added rigidity, one additional wire was bounded to six wires to form a mesh. This assembly allows the sample to strain freely in all direction.

The test specimen was pierced before being mounted onto the grips securely and then the grips and specimen assembly was mounted onto the testing apparatus. The grips were identical in size and shape, thus no misalignment occurred. Nonetheless, the image was taken from the center of the specimen to ensure the grips did not affect the experimental data.

Before the actual test, the preconditioning test was performed to minimize the viscoelastic response of the specimen. The preconditioning test consists of a series of cyclic loads applied to the sample, normally (not necessarily) in the same strain rate and stretch ratio of the tension test that is going to be performed afterwards. As seen in the Figure 4. 2, the first cycle is totally separated from the other cycles which means that after the fourth cycle the viscoelastic properties of the material is almost constant and the

specimen is ready for the test. The preconditioning test in this experiment is performed over 4 cycles.

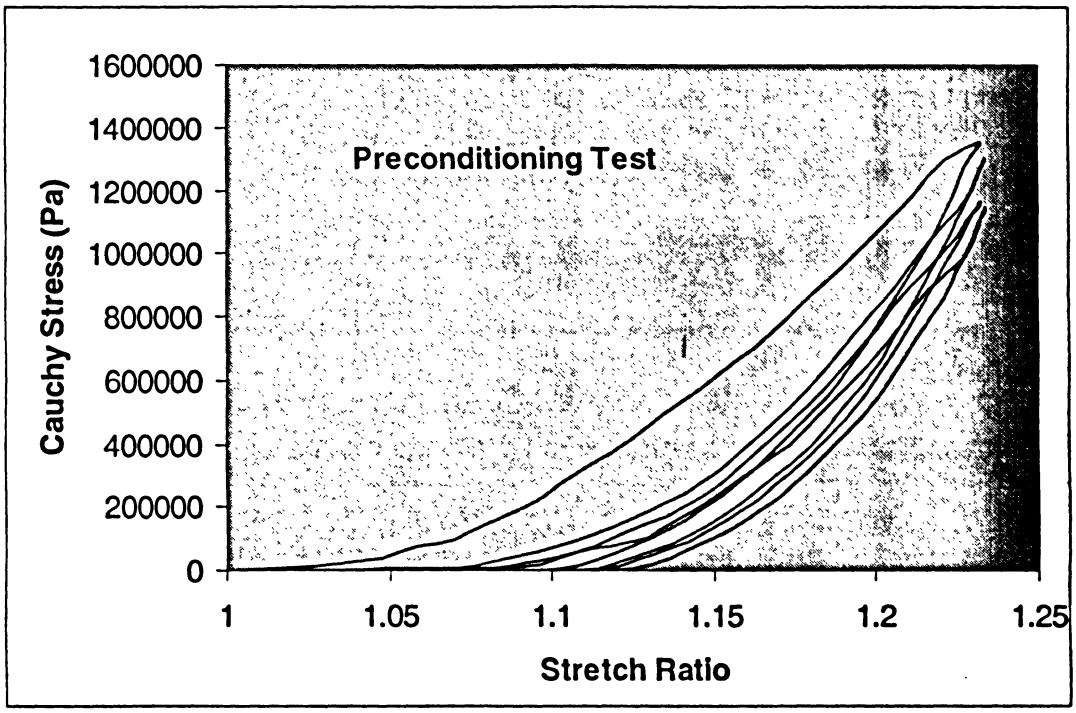

Figure 4. 2 Preconditioning test

The uniaxial test was performed at 0.75mm/s strain rate and three different stretch ratios (elongation divided by initial length of the sample): 1.2, 1.3 and 1.4. These stretch ratios are based on the displacement of the grippers, calculated by the rotation of the step-motors and it is not the real elongation of the sample. The real elongation was calculated based on the pictures obtained from the camera. The data collection rate was variable between 1.5 to 3 Hz. The images and data were taken at exactly the same time. After reaching the maximum strain, the sample was held at maximum strain to study how the stress relaxes (Figure 4. 3) even though investigating the relaxation behavior was not a part of this study.

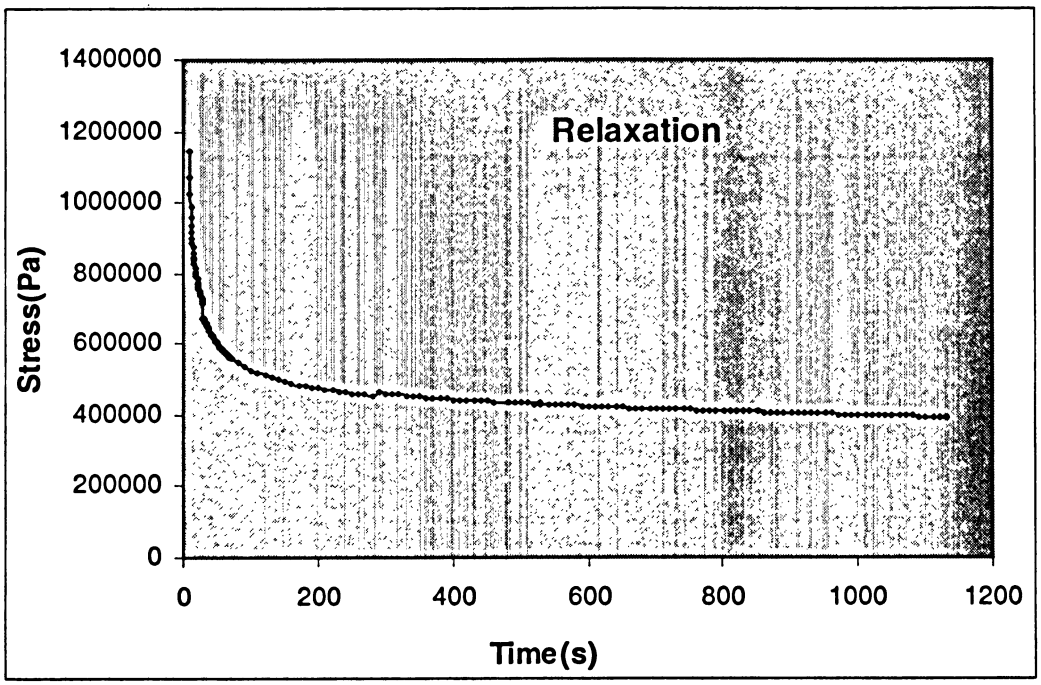

Figure 4. 3 Stress relaxation graph

The strain at the center of the specimen was measured by drawing a 5mm x 5mm square section on the center of the specimen using enamel ink. A reference digital image was taken from the sample before the moving of the grips starts. Then the consequent digital images were used to compare the stretch with the reference image. The determination of stretch ratios was made after the test protocols were completed. A commercial package, EasyAccess eVision 6.2 by Euresys, was used to measure the local strain or stretch ratio experienced by the specimen. Briefly, first the grey scale transition parameters were set so that the transition between black-white-black could be recognized. The software then measured the number of pixels between each black to white transition and shows it on the screen using a chart. In the image, each pixel had a specific size that can be used to convert the measurement from number of pixels to a standard unit of measurement. Figure 4. 4 shows the sample with the square in the software. By dividing the distance

between two points by the distance at the beginning, the stretch ratio is obtained. This method was used to determine the in-plane stretch ratio or strain.

Stretch ratio or strain through the thickness cannot be directly measured during the test. However, assuming incompressibility, one can determine the strain trough thickness from in plane strain. The assumption of incompressibility ensures a constant volume in which case, the stretch ratio through thickness can be determined from the following equation.

$J = \lambda_1 \lambda_2 \lambda_3$ where J is the Jacobian of deformation **Eq. 4. 1**

For an incompressible material, the Jacobian of the deformation is one. Therefore, with simple algebraic manipulation, the through the thickness stretch can be determined from the following relation [58]:

$$\lambda_3 = \frac{1}{\lambda_1 \lambda_2}$$ **Eq. 4. 2**

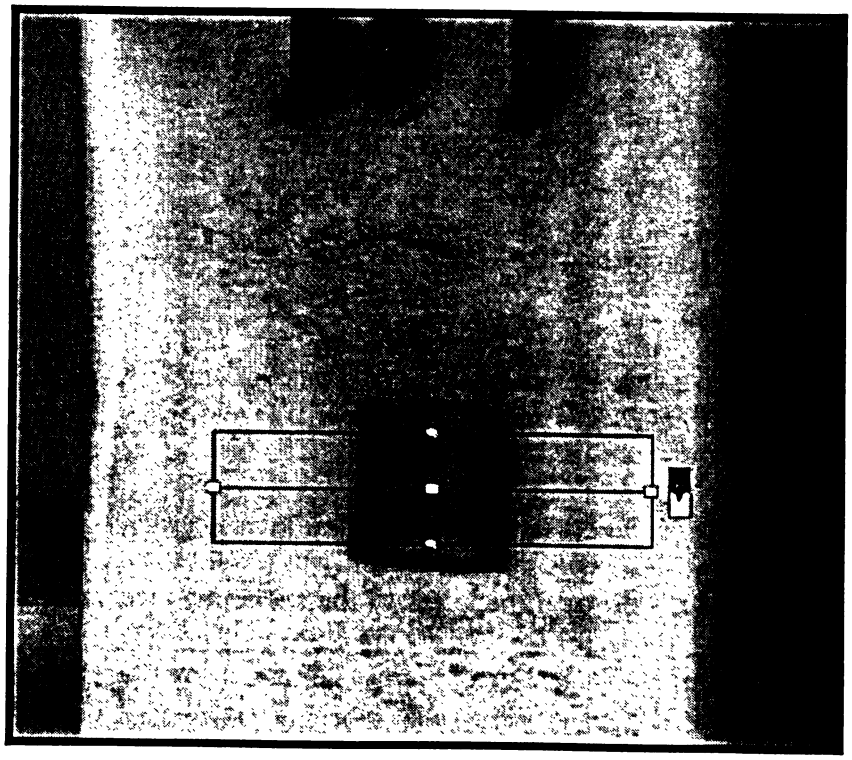

Figure 4. 4 Strain measurement

One of the issues in performing the experiment was measuring the initial length and width of the sample. This cannot be done before mounting the sample since a preload is applied to establish a reference point. This preload may cause stretch at rest configuration. Therefore, the initial length should be measured after mounting the sample. Before beginning the test, a ruler was located beside the sample and an image was taken, this allows the determination of original sample length (Figure 4. 5).

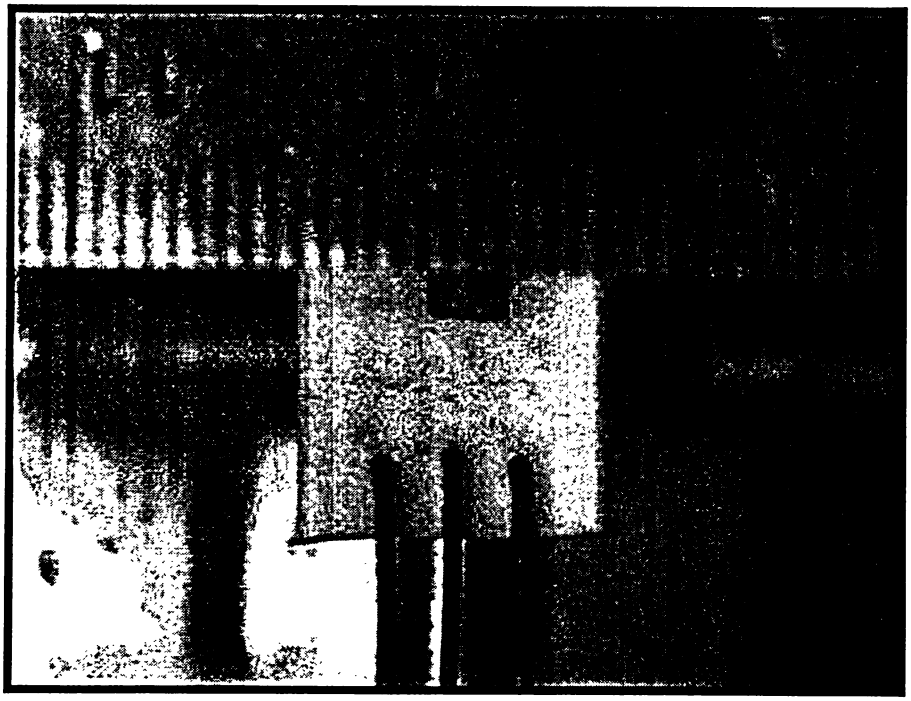

Figure 4. 5 Measuring the width of the sample

In order to determine the Cauchy stress, the instantaneous cross sectional area must was determined. At first, the initial cross-sectional area of the sample was calculated from the in-plane dimension and the original thickness of the specimen measured using an optical micrometer. The subsequent instantaneous cross sectional area at each load increment was calculated from the instantaneous in-plane dimension and the thickness determined based on the assumption of incompressibility.

The force applied in each direction is measured by means of load a transducer. Thus, having the force and instantaneous cross-sectional area, stress can be calculated. The stress calculated by this method is the Cauchy or true stress, because it is the force divided by the instantaneous cross sectional area, not the initial one.

4.3 Results

For each test protocol, a graph of Cauchy stress versus stretch ratio was obtained. The Cauchy stress and stretch ratio were calculated as explained above. In the Figure 4. 6 to Figure 4. 8 Cauchy stress versus stretch ratio is seen for each test.

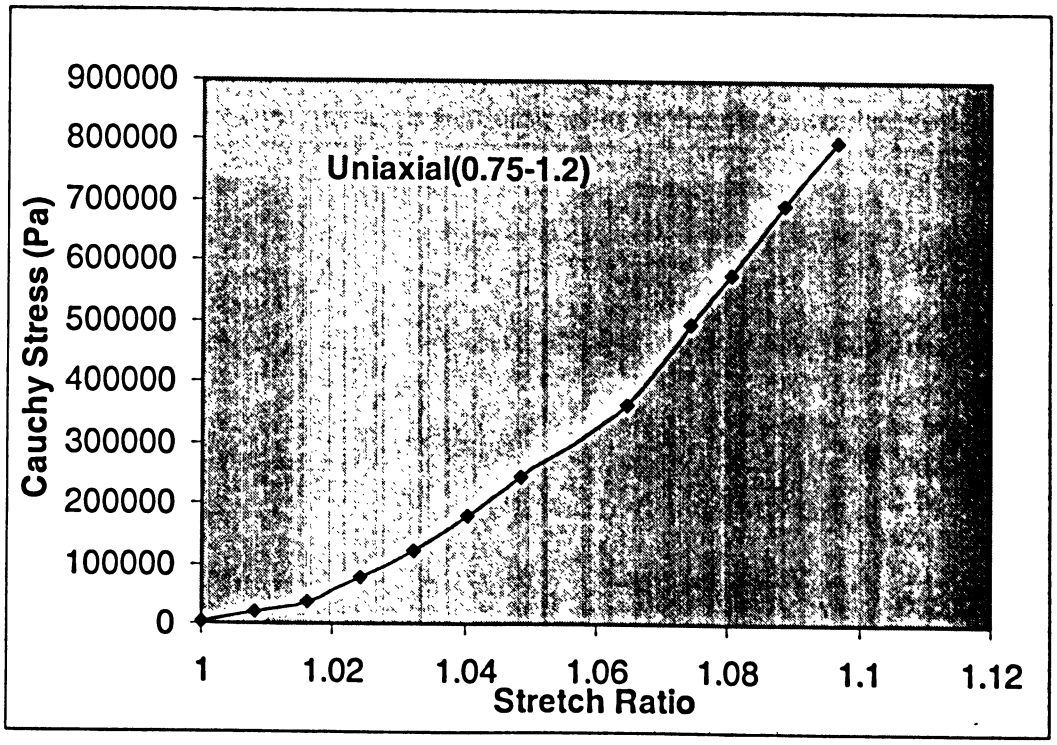

Figure 4. 6 Cauchy stress versus stretch ratio (strain rate: 0.75 mm/s, stretch ratio: 1.2)

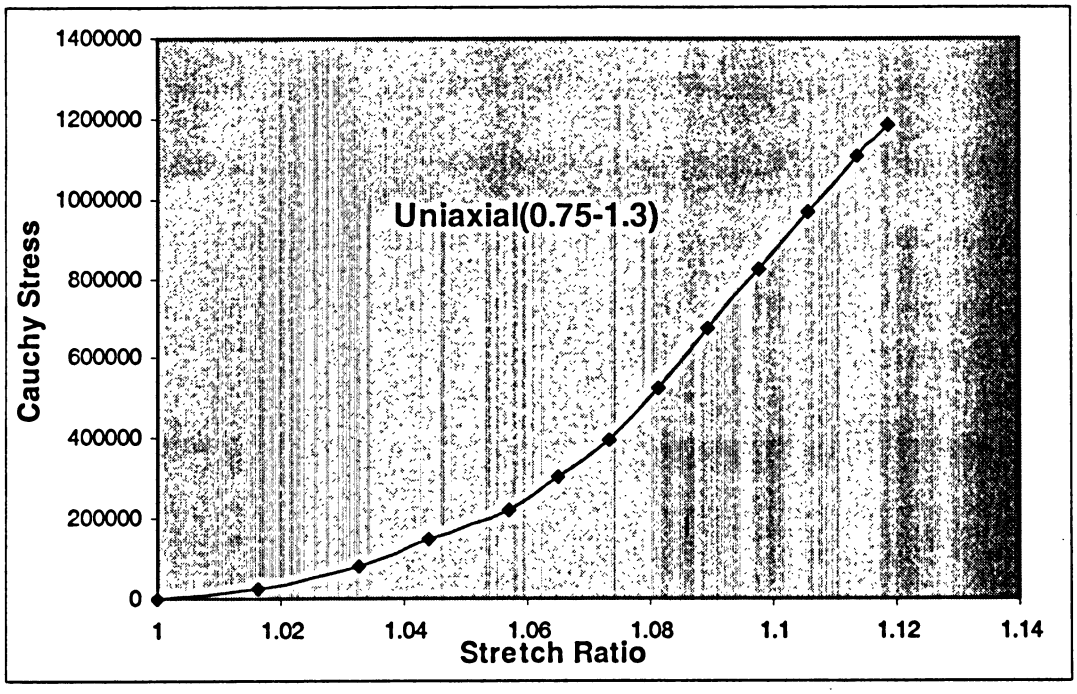

Figure 4. 7 Cauchy stress versus stretch ratio (strain rate: 0.75 mm/s, stretch ratio: 13)

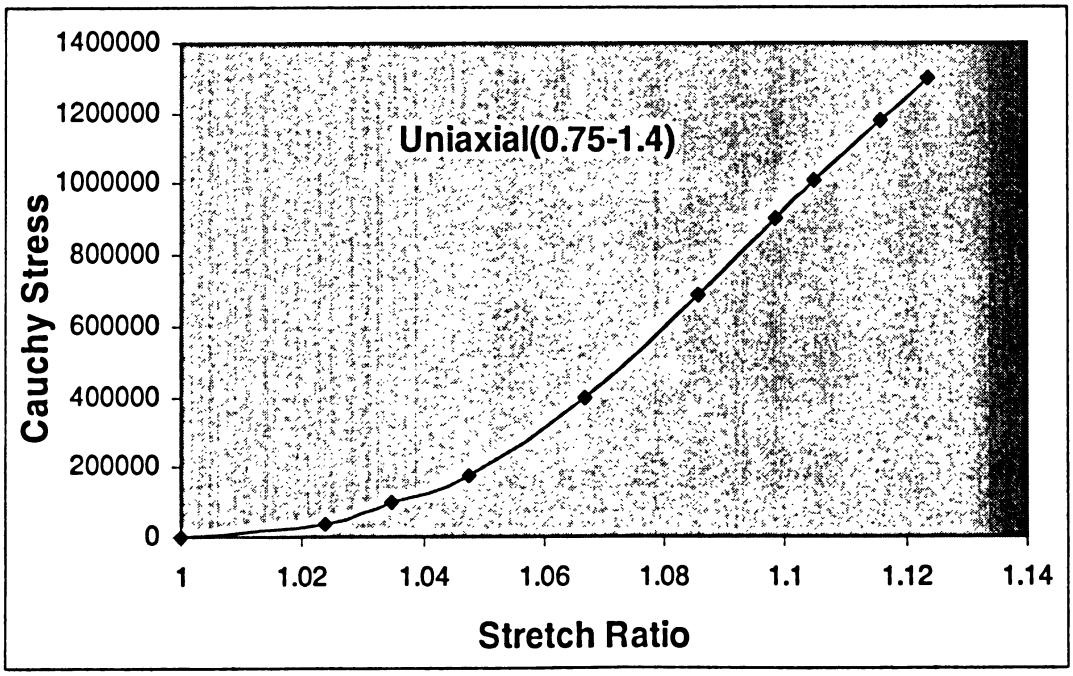

Figure 4. 8 Cauchy stress versus stretch ratio (strain rate: 0.75 mm/s, stretch ratio: 1.4)

The responses of the different test specimen to uniaxial test protocol were the same. These graphs all have a characteristic in common. In all the graphs, we see that the

stiffness of the cartilage in tension depends on the stretch ratio. In all test protocols, the materials responded with a shallow slope in the low strain regions followed by sudden increase to the slope of the stress stretch graph.

As it has been mentioned, the cartilage was assumed to be a linear, isotropic and perfectly elastic material. As such, the least squares method of optimization was used to determine the slope of the linear approximation of the experimental data. In all cases the modulus of elasticity of the material is approximately 3.7 MPa which is in close agreement with the reported values in the published literature. However, it is important to note that there is a wide variation in the published data in the literature. The modulus of elasticity of cartilage has been reported to vary from 3.4 to 3.8 MPa, however as low as 3.2 MPa and as high as 10 MPa has been reported as well [6, 29]. Generally, the modulus of elasticity obtained from these experiments seems reasonable as compared to the published results form other experiments.

The Poison's ratio, which is the ratio of lateral strain to axial strain, was calculated in each test as well. In the first, second and third tests the Poisson's ratio was found to be 0.41, 0.31 and 0.35 respectively. Taking an average the Poisson's ratio used in the FE model was 0.37 which is in good agreement with the value 0.45, reported by Yagonandan et al. [59].

5 Finite Element Modeling of Vertebrae and Intervertebral Disc

5.1 Introduction

The finite element method is particularly suitable for the stress analysis of complex structures. Taking into account the disc geometry and the material properties, the exactness of the preprocessing has a great and direct impact on the final outcomes. The preprocessing step is mainly generating the geometry, assigning the material properties and applying the boundary conditions.

In this chapter, the modeling, meshing, applying the boundary conditions and solving the model of C3-disc-C4 using commercial software is explained. The results of the FE analysis are presented and the comparison of the numerical results with published data is presented. As a result of the method of generating the model, the geometry of the system in this model is highly precise and hence the results of the FE simulation would not be affected by lack of accuracy in the geometry.

In this work, only the C3 and C4 vertebrae, the cartilage disc between C3 and C4, and the ligaments connecting C3 and C4 were modeled. The effects of the other components of the spine that are in touch with vertebrae (tendons, disc above C3, etc.) are all included in as boundary conditions (loads and constraints).

5.2 Generating the FE Model

A 32,000 point model that represents a life-size human C3, C4 and cartilage between C3 and C4 was purchased. A software package called Hypermesh was used to generate surfaces from data points. Briefly, to accurately model C3, 20 surfaces were generated. Equally, 22 surfaces were generated through the data points to model C4 and 5 surfaces were generated to model the cartilage. The surfaces defining each component were transferred to FE a software package called MscMarc. Using this commercial software, each surface was converted into triangular elements. Since each component consisted of multiple surfaces, the common boundary of every two touching surface were connected manually. Performing this process, a closed form surface mesh of each component was modeled. Once the surface mesh was modeled, it was converted to solid four node tetrahedral elements. The following table summarizes the number of element of each component.

Component	C3	C4	Nucleus Pulposus	Annulus Fibrosus
Number of Element	17248	15309	910	4922

Table 5. 1 Number of elements

As it was explained in chapter 2, in human anatomy, the ligaments contribute to the overall load carrying capacity of vertebrae. To this end, link elements were used to model the ligaments introduced in chapter 2 to include the effect of these components on the mechanical response of C3- C4 to external loading. The modulus of elasticity and the Poisson's ratio of ligaments were adapted from Yoganndan et al. [2] (see Table 5. 2).

Component	E(MPa)	Cross Section(mm^2)
Anterior Longitudinal Ligament	43.8	11.1
Posterior Longitudinal Ligament	40.9	11.3
Interspinous Ligament	4.9	13.0
Ligamentum Flavum	3.1	46.0
Capsular Ligament	5	42.2

Table 5. 2 Ligament material properties [2]

The 4 node tetrahedral element was chosen since the vertebrae geometry is very complex. This is a four-noded element with a linear shape function. The shape functions are expressed with respect to the area coordinate. The stiffness is calculated using a single point at the centroid of the element.

The surface elements were then converted to solid elements by expansion of the shell elements; the solid meshes were then locally refined and redefined wherever distortion was apparent. This procedure was repeated until the elements with bad aspect ratio or distorted elements were eliminated. The aspect ratio is defined as the ratio of the largest and smallest dimension of an element. If the aspect ratio exceeds 5, excessive deformation can result. Excessive deformation causes element-inside-out or complete

collapse of element, which can cause analysis failure. This procedure was followed for each component in this analysis. Figure 5. 1 to Figure 5. 4 show the FE model of C3, C4 and the cartilage between the C3-C4 bones. Figure 5. 1 depicts the complete model and Figure 5. 2 depicts the cartilage. Figure 5. 3 depicts the model showing contact surfaces and the boundary conditions and Figure 5. 4 shows the different components in the model using different colors.

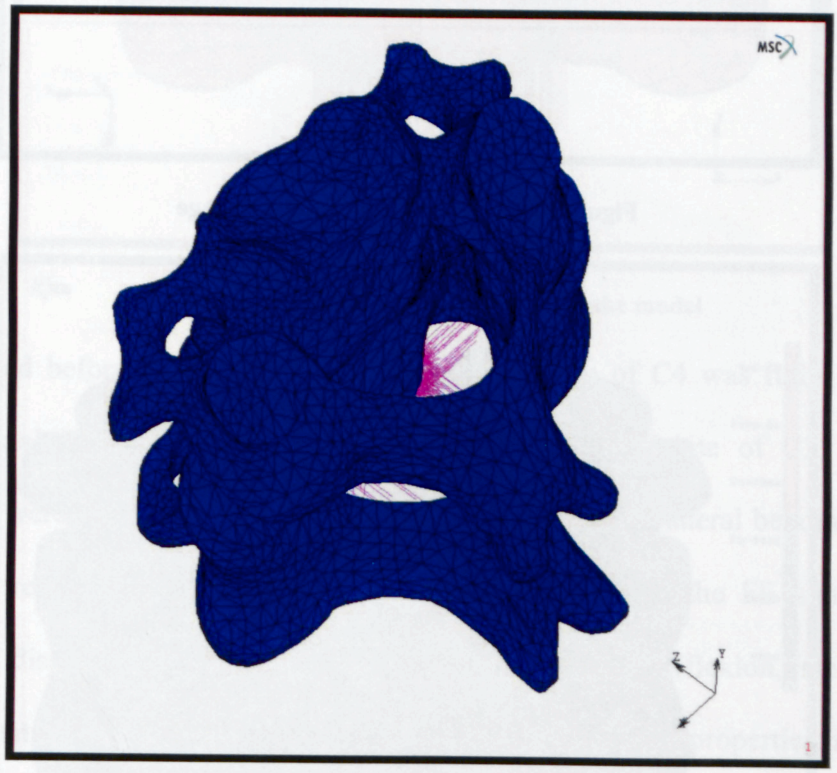

Figure 5. 1 The entire FE model

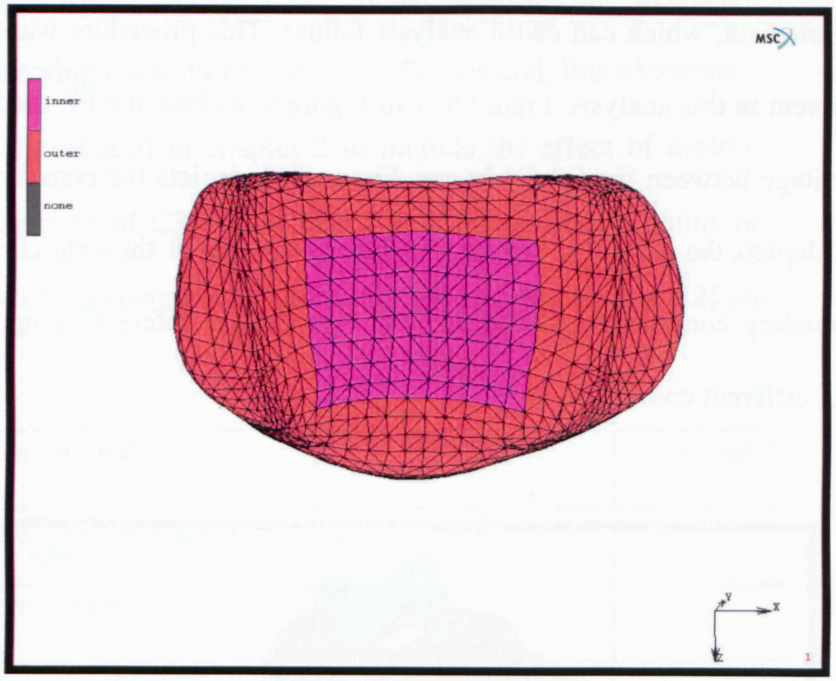

Figure 5. 2 The FE model of the cartilage

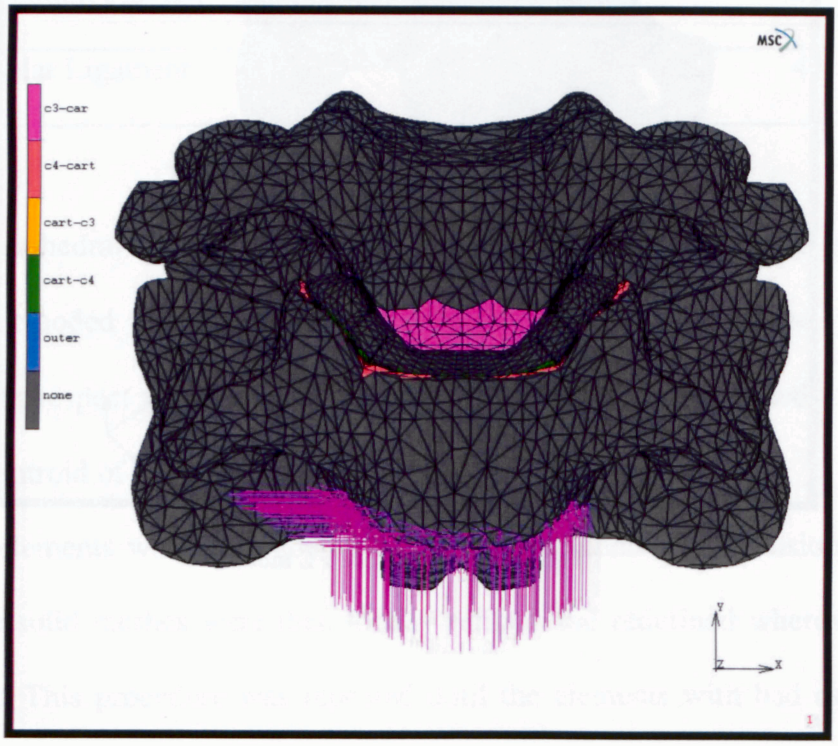

Figure 5. 3 The Contacts and the boundary conditions

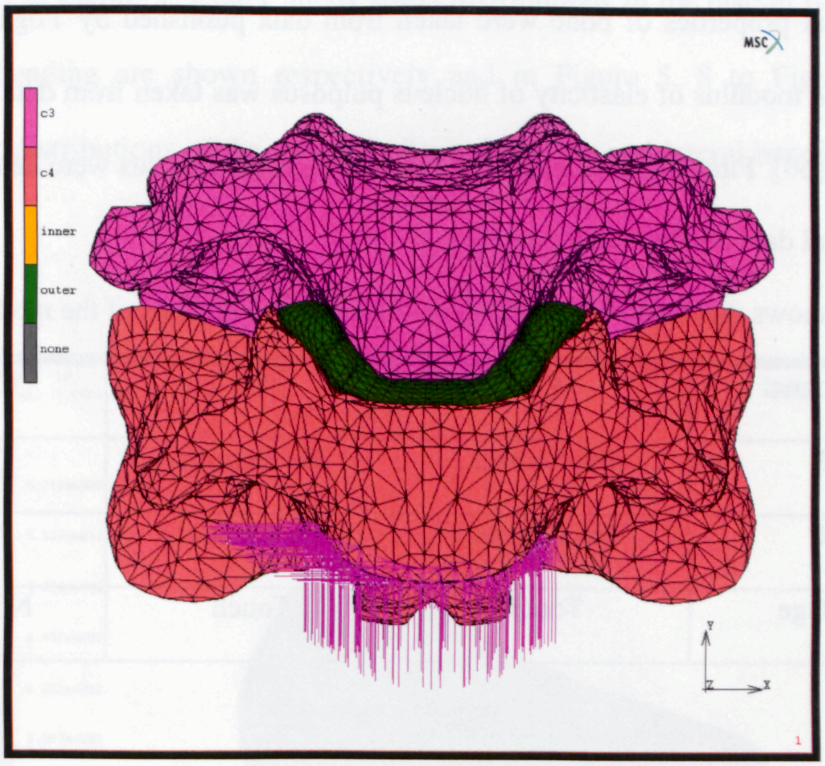

Figure 5. 4 The different components in the model

As mentioned before, in the model the inferior endplate of C4 was fully constrained. Then an axial load of 74N was applied to the upper endplate of C3. Then three simulations were run and pure moments of 1.8Nm (in flexion, lateral bending, and axial rotation) were applied to the superior endplate of C3. From the FE simulation, the rotation and displacement of C3 under different load conditions (flexion, lateral bending, and axial rotation) were calculated. Table 5. 3 shows the material properties implemented in the FE model for each component except for ligaments which were already shown.

Component	Cortical Bone	Interior of Bone	Nucleus Pulposus	Annulus Fibrosus
Modulus (MPa)	10000	1000	1	3.7
Poisson's Ratio	0.3	0.3	0.49	0.37

Table 5. 3 Meterial properties in the FE model [60, 61]

The material properties of bone were taken from data published by Yoganandan et al. [59] and the modulus of elasticity of nucleus pulposus was taken from data published by Goel et al. [60]. Finally the material properties of annulus fibrosus were determined from experimental data obtained in this study.

Table 5. 4 shows the contact types between different components of the model.

Component	C3	C4	Cartilage
C3	No Contact	No Contact	Touch
C4	No Contact	No Contact	Touch
Cartilage	Touch	Touch	No Contact

Table 5. 4 Contacts table

5.3 Validation of the Model and Results

To ensure that the process of modeling and assigning experimentally determined material properties to various components of the cervical spine were accurate and suitable, the FE model of C3-C4 ws validated by the reported results in the literature.

To validate the FE model, the results are usually compared to the experimental results found in the literature suitable for validation. A reasonable agreement between the simulation results and published data is considered validation of the model. As the model is validated the results of the analysis can be used in further analyses.

In this part of study the model was validated with the published experimental data of Moroney et al. [61]. The boundary conditions were set at the values reported in this paper. The stress and strain contour plots of each solution are presented. Figure 5. 5 to Figure 5. 10 show the FE results.

In Figure 5. 5 to Figure 5. 7 the Cauchy stress distributions in the disc in flexion, torsion and lateral bending are shown respectively and in Figure 5. 8 to Figure 5. 10 the displacement distributions of the model in flexion, torsion and lateral bending are shown respectively.

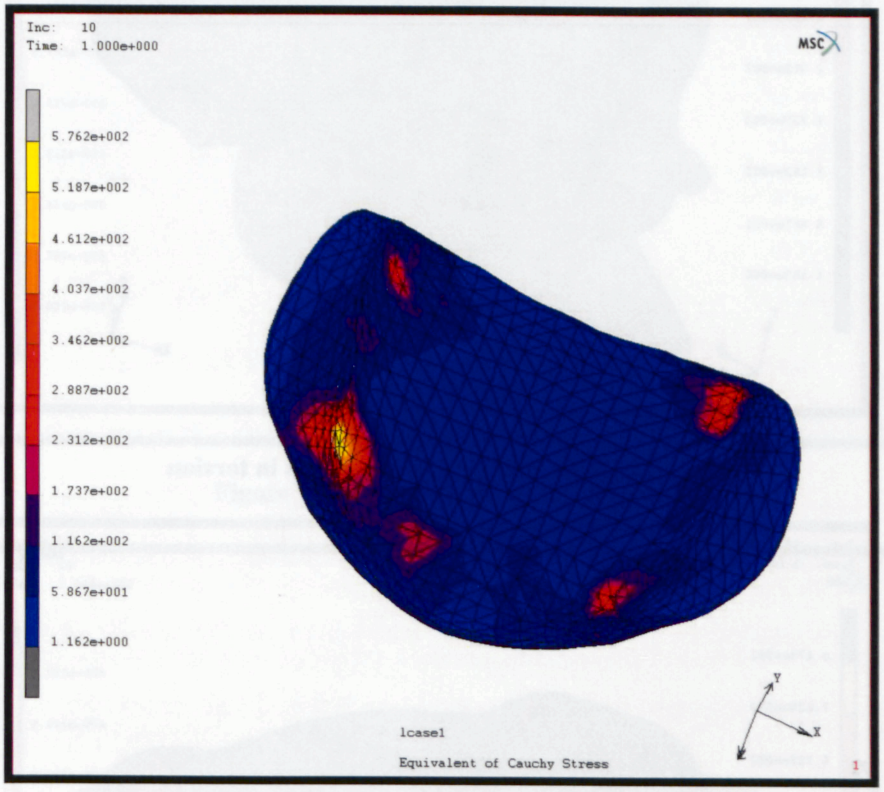

Figure 5. 5 Cartilage Cauchy stress in flexion

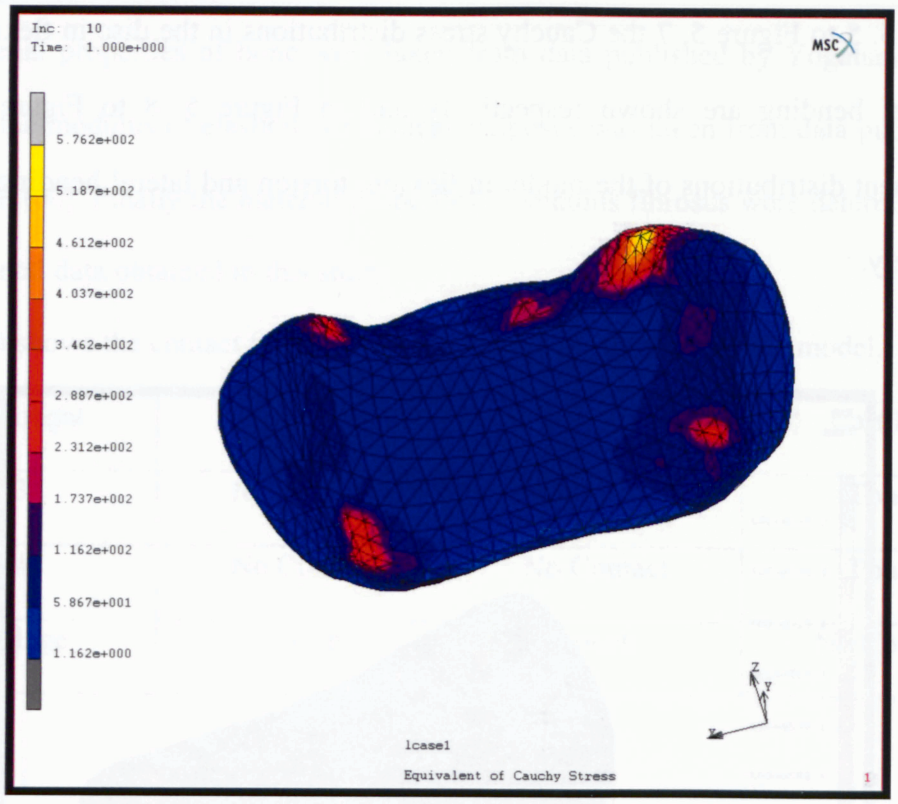

Figure 5. 6 Cartilage Cauchy stress in torsion

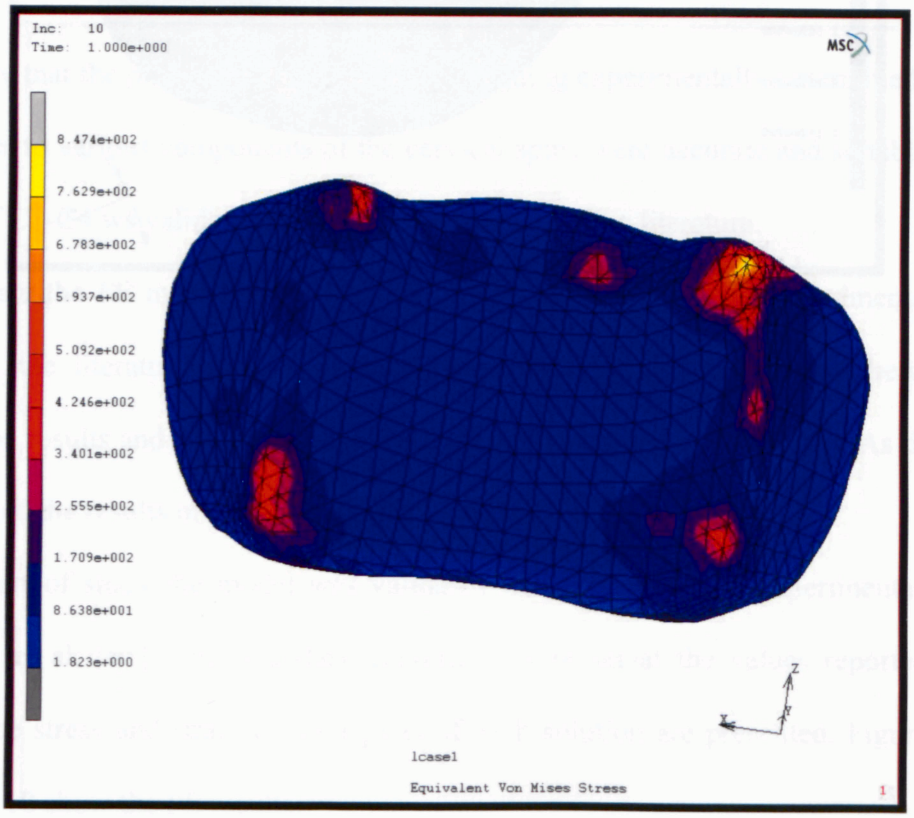

Figure 5. 7 Cartilage Cauchy stress in lateral bending

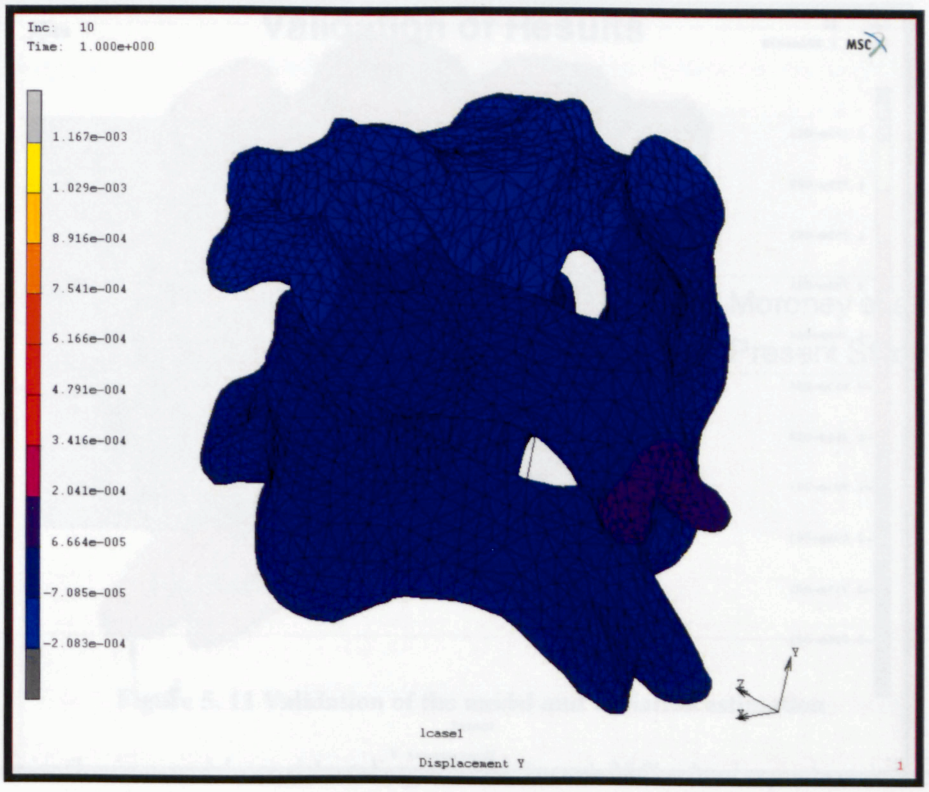

Figure 5. 8 Displacement field in flexion

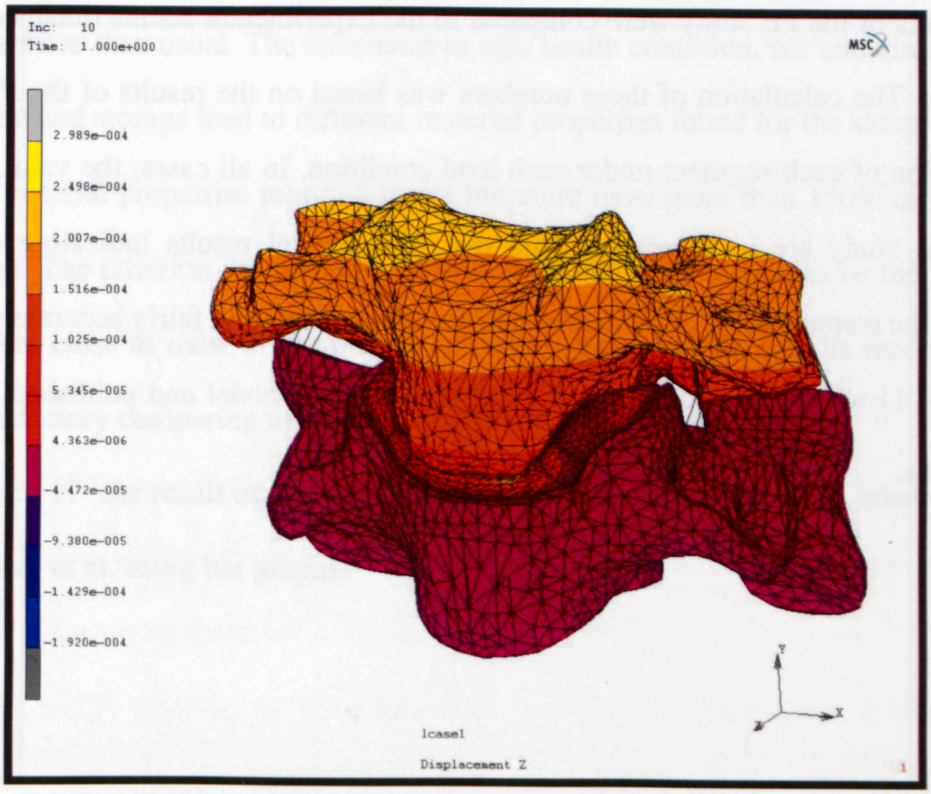

Figure 5. 9 Displacement field in torsion

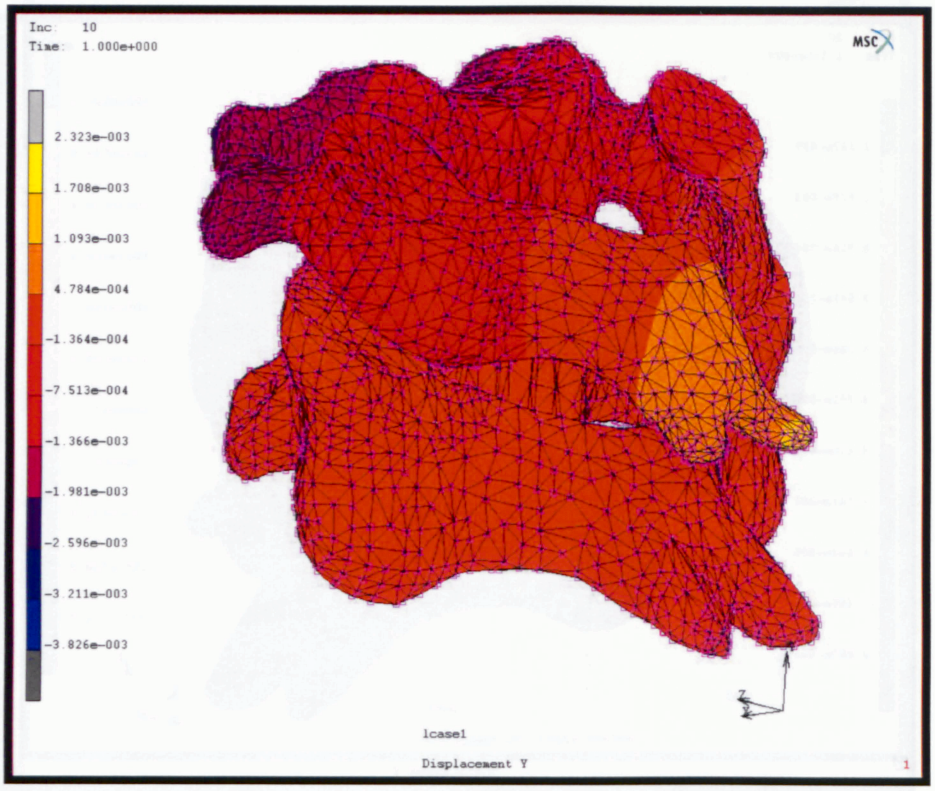

Figure 5. 10 Displacement field in lateral bending

The results of the FE study were compared to the experimental results obtained from the literature. The calculation of these numbers was based on the results of the FE analysis for rotation of each segment under each load condition. In all cases, the values obtained from this study are in agreement with the experimental results indicating our model predicts the response of C3-cartilage-C4 to the external loading fairly accurately.

Figure 5. 11 shows the error and variation between our model and published data using bar graphs.

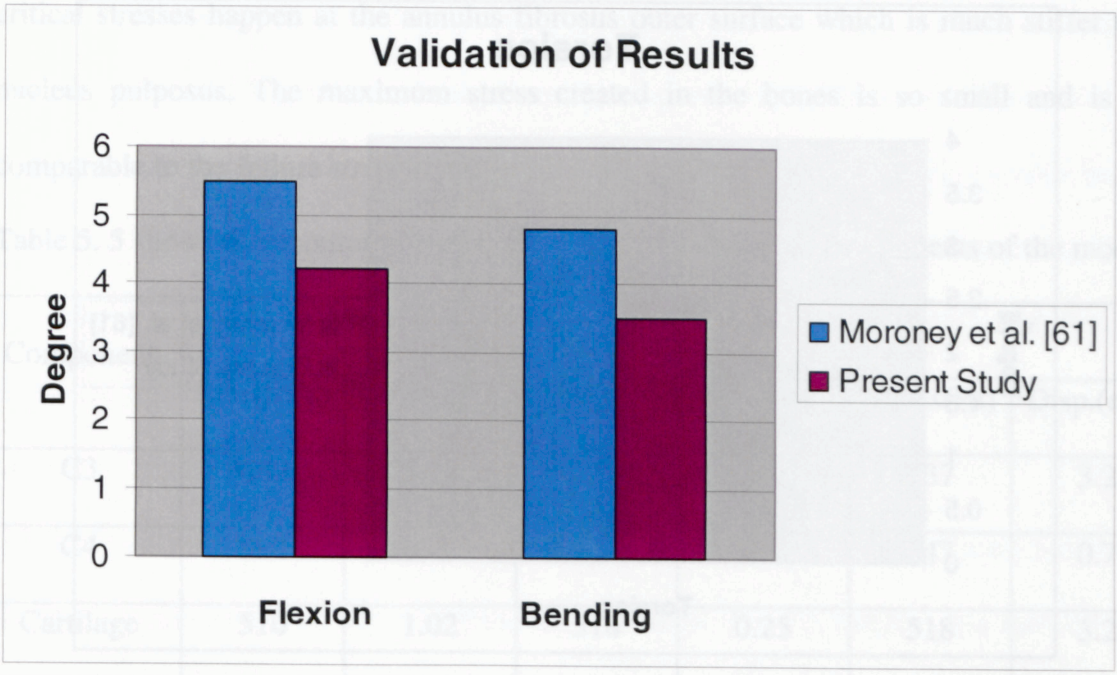

Figure 5. 11 Validation of the model and variation estimation

The errors in flexion and lateral bending are 24% and 33%. An important issue to notice here is that in biomechanical studies because of the differences in samples normally the errors are more than usual. The difference in age, health condition, sex and circumstances of excision and storage lead to different material properties found for the sample. For this fact, the material properties reported in the literature have more than 150% difference to each other. The criterion for material properties in this study is tried to be the properties which were close to most of the published values. Therefore the results reported above seem satisfactory comparing to the results in the literature.

In Figure 5. 12 the result of the simulation in torsion is compared to the results reported by Moroney et al. using bar graphs.

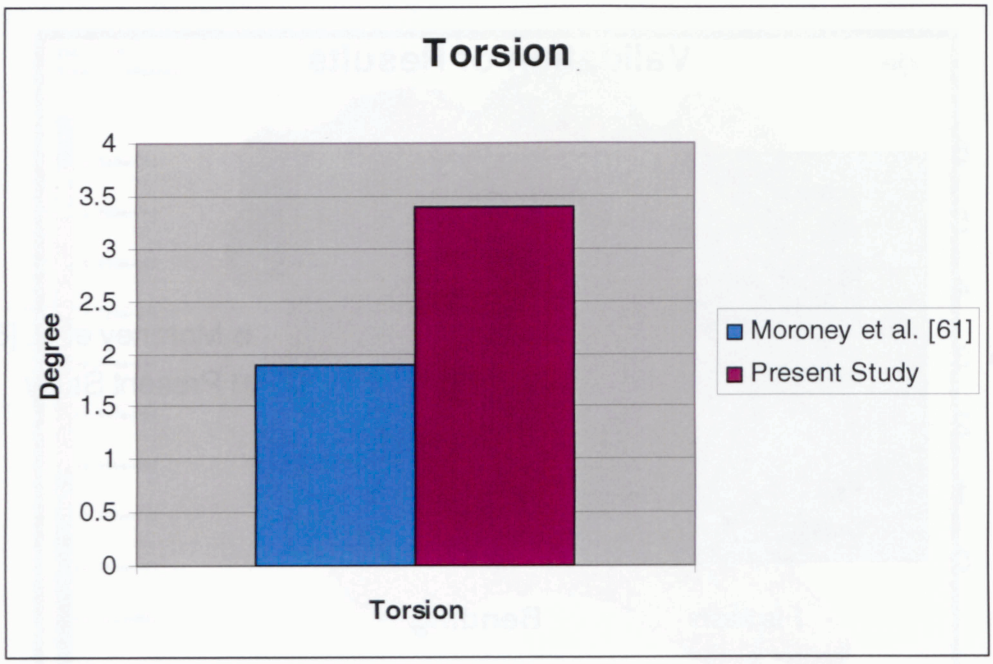

Figure 5. 12 Eror in torsion

The error in torsion seems too large when compared with the errors of flexion and bending. The fact that in torsion, most of the stress is shear stress and the fibrous structure of intervertebral disc coupled with the assumption of linear isotropy in the disc might be the reasons of such a large error.

Another point that needs extra attention is the comparison of the maximum stress in the model to the failure stress of the cartilage. One of the main reasons of this study was to examine whether the loading conditions considered here cause permanent damage or complete rupture of the cartilage.

Moroney et al. [61] have reported that normally, failure does not occur below the rotation of 10 degrees or 3.1 Nm moment and the disc (annulus fibrosus) fails at strains value of 20-35%. The maximum stress in the results obtained in the finite element model is about 10 KPa which is much less than reported failure stress of the cartilage (750 KPa). As seen in the contour plots, in all cases the maximum stress in disc occurs in the corners. These

critical stresses happen at the annulus fibrosus outer surface which is much stiffer than nucleus pulposus. The maximum stress created in the bones is so small and is not comparable to the failure stress of the bone.

Table 5. 5 shows the maximum stress and displacements in the components of the model.

Component	Mx		My		Mz	
	Stress(Pa)	Disp.(mm)	Stress(Pa)	Disp.(mm)	Stress(Pa)	Disp.(mm)
C3	660	1.02	737	0.25	737	3.2
C4	990	0.067	947	0.05	947	0.7
Cartilage	510	1.02	518	0.25	518	3.2

Table 5. 5 Maximum stress and displacements in the components of the model

6 Conclusion and Future Work

The objective of this study was twofold: firstly to carry out an experiment on bovine knee cartilage and obtain the material properties, secondly to implement the mechanical properties of cartilage in a FE model of human cervical spine and validate the method of study by comparing the results to the results reported in the literature.

The anatomy of cervical spine, especially the anatomy of vertebra and intervertebral disc as well as their material structure and properties was studied to provide sufficient data about the structure of the model being analyzed. This was essential as our focus was to construct an FE model as accurate as possible.

Several articles about the research works relevant to this topic were studied and different methods by which biomechanical engineers have worked in this area were examined. The

protocols of testing the cartilage used by many researchers were studied in detail to design the best test protocol possible, considering our capabilities and objectives. The Cauchy stress was determined using the experimental data obtained during tensile testing and from this a data regression analysis was conducted to determine the modulus of elasticity of cartilage based on the material response. The error of modulus of elasticity found for the cartilage by this method has error value of -15% to 68% when compared to the values reported in the literature, but it is close to most of them.

FE analysis, as a powerful method in analyzing physical models, has always been one of the best possible ways to solve engineering problems. The FE method is a method used by many researchers to study biomaterials under various loadings. The challenging part in this method is the determination of the material properties and geometry and researchers normally use the medical literature to create the geometry of the organ under investigation. The experimental method is carried out on sample tissue to determine the bulk properties and these properties are implemented in the FE model.

In this work, a three-dimensional linear FE model has been developed to analyze C3-C4 vertebra under applied moments. The surface model of C3 and C4 was purchased and the author used this surface to generate the FE model. The material properties of the cartilage were obtained from the experiment and were validated against the published data by using the bovine knee cartilage as human intervertebral disc. The FE simulation satisfactorily predicts the response of C3-C4 under boundary loading conditions.

This study shows that the resemblance in structure in fibrocartilage of intervertebral disc and knee joint leads to similar mechanical characteristics. Therefore assuming the equality between the mechanical properties of two live tissues that have similar structures

is a safe assumption. Disc implantation is the topic of many studies and this fact can be an initial step in fabricating all artificial tissues, including cartilage.

Using nonlinear material properties as opposed to linear material properties may be the next step to improve the results.

Linearity of the disc tissue was one of the main assumptions in this study. In fact, the stresses vs. strain graphs obtained from experiments were nonlinear. In the diagram the range of strain that the cartilage normally encounters is the linear range of stress strain curve. For this reason, the linearity assumption was considered valid for this study.

Another assumption that was made to simplify the analysis was to consider the cartilage as isotropic. In reality, because of fibrous structure, cartilage is anisotropic. However, in many cases various authors have assumed the cartilage is isotropic and their results were acceptable and reliable, so in this study this assumption was adopted as well. Furthermore, assuming the orthotropy means that there is a need for nine independent variables to form the modulus of elasticity tensor. To obtain these variables the material should be tested in many directions simultaneously which was not attainable as far as most biological tissues are concerned. Simulating an orthotropic model may reduce the error caused in torsion.

Therefore, important improvement in this study can be made at the experimental stage by carrying out a biaxial test with which some orthotropic properties of the cartilage can be measured and applied in a FE model for realistic and accurate analysis.

The two above changes in the model can lead to a better and more accurate result but it is very important to keep in mind that solving a nonlinear anisotropic model with such a complicated geometry and so many contacting components may increase the solution

time drastically or may even make it unattractive since the accuracy achieved does not justify the computing time.

Another step to improve this study is to test a tissue closer to human intervertebral disc which may be bovine cervical disc. Testing a human intervertebral disc is a complicated endeavor which needs powerful medical equipment and a medical team to work alongside the biomechanical engineers to carry out a safe, ethical and right method in testing. In addition, the availability of the sample can be an obstructing issue. But testing the intervertebral disc of a bovine is more feasible because of the availability and the larger size of the sample available. The results of the study prove that knee joint cartilage can be used instead of intervertebral disc in the experiment to measure its mechanical characteristics.

Improving the grips may have a good effect on the results of the study too. The advantage of the grips of the experiment was the possibility for the sample to have transverse strain freely. This characteristic was the main reason for using piano wires rather than clamps or glue. But mounting the sample on the grip was not an easy task and improving the grips may solve this problem.

In the experiment carried out in this study the curves of the preconditioning and creep were obtained but not investigated. Working on viscoelastic and creep behavior of the material can be another good further step in this study.

REFERENCES:

[1] Y.C. Fung, "Biomechanics, Its Foundations and Objectives", Prentice-Hall, 1972.

[2] N. Yoganandan, S. Kumaresan, "Biomechanics of the cervical spine Part 2. Cervical spine soft tissue, responses and biomechanical modeling",Clinical Biomechanics 16 (2001) 1-27.

[3] <http://supplementnews.org/cartilage/> 19 Aug. 2006.

[4] <http://en.wikipedia.org/wiki/Cartilage> 22 Aug 2006.

[5] A . S.A ravind , R . K . Saxerrat, "Influence of loading on the biomechanical properties of the articular cartilage", Proceedings RC-IEEE-EMBS & 14th BMESl – 1995.

[6] Ulrich Hansena, Spyridon Masourosb, "Material properties of biological tissues related to joint surgery", Current Orthopaedics (2006) 20, 16–22.

[7] <http://en.wikipedia.org/wiki/Vertebra> 22 Aug 2006.

[8] <http://www.alphaklinik.com> 12 Jan 2007.

[9] <http://education.yahoo.com/reference/gray/subjects/subject?id=20>7 Jan. 2007.

[10] <http://www.back.com/anatomy-lumbar.html>12 Jan 2007.

[11] <http://en.wikipedia.org/wiki/Vertebral_column>22 Aug 2006.

[12] <http://www.harms-spinesurgery.com/src/plugin.php?m=harms.ANA05E>23 Aug. 2006.

[13] <http://www.chirogeek.com/000_Disc_Anatomy.htm>23 Aug. 2006.

[14] <http://www.spineuniverse.com/displayarticle.php/ >24 Aug. 2006.

[15] <http://www.spineuniverse.com/displayarticle.php/article1023.html>Jan. 12 2007.

[16] Kotani, Yoshihisa Abumi, Kuniyoshi Shikinami, Yasuo Takahata, Masahiko Kadoya, Ken Kadosawa, Tsuyoshi Minami, Akio Kaneda, Kiyoshi, "Two-year observation of artificial intervertebral disc replacement: results after supplemental ultra-high strength bioresorbable spinal stabilization", Journal of Neurosurgery : Spine, 2004.

[17] Abhijeet Joshia, Garland Fussellb, "Functional compressive mechanics of a PVA/PVP nucleus pulposus replacement", Biomaterials 27 (2006) 176–184.

[18] Hirokazu Mizuno, Amit K. Roy, "Biomechanical and biochemical characterization of composite tissue-engineered intervertebral discs", Biomaterials 27 (2006) 362–370.

[19] S.C. Fan, D.N. Ghista, "Biomechanics of the Intrinsically Optimal Design of the Intervertebral Disc", Proceedings of the 2005 IEEE Engineering in Medicine and Biology 27th Annual Conference Shanghai, China, September (2005) 1-4.

[20] Peter Evans, Binil Starlyb, "Computer Aided Tissue Engineering Design for a Spinal Intervertebral Disc", IEEE, 2005.

[21] Lawrence M. Boyd "Design and Testing of an Intervertebral Disc Prosthesis", Proceedings - 19th International Conference - IEEE/EMBS, 1997.

[22] JP WU, TB Kirk, "Study of shape change of sheep Chondrocytes with application of compression to cartilage", New Zeland Information System Conference, (2001), 18-21.

[23] Rani Roy, Sean S. Kohles, "Analysis of Bending Behavior of Native and Engineered, Auricular and Costal Cartilage" Proceedings of the IEEE 27th Annual Northeast Bioengineering Conference, (2001), 31-32.

[24] Paul C. Ivancic, Manohar M. Panjabi, "Cervical Spine Loads and Intervertebral Motions During Whiplash", Traffic Injury Prevention, 2006, 7:389–399.

[25] P. C. Ivancic Manohar, M. Panjabi, "Biofidelic whole cervical spine model with muscle force replication for whiplash simulation", Eur Spine J (2005) 14: 346–355.

[26] Manohar M. Panjabi, "Clinical spinal instability and low back pain" Journal of Electromyography and Kinesiology 13 (2003) 371–379.

[27] Orin K. Atlas, Seth D. Dodds, Manohar M. Panjabi, "Single and incremental trauma models:a biomechanical assessment of spinal instability", Eur Spine J (2003) 12 :205–210.

[28] M.M. Panjabi, J. Cholwicki, K. Nibu, "Critical load of human cervical spine, an in vitro experimental study", Clinical Biomechanics, Vol. 13, No.1, 1998, 11-17.

[29] Kenneth R. Gratz, Van W. Wong, "Biomechanical assessment of tissue retrieved after in vivo cartilage defect repair: tensile modulus of repair tissue and integration with host cartilage", Journal of Biomechanics, 2006, 138–146.

[30] Andreas Haisch, Georg N. Duda, "The morphology and biomechanical characteristics of subcutaneously implanted tissue-engineered human septal cartilage", Eur Arch Otorhinolaryngol, 2005, 993–997.

[31] Ramaswamy Krishnan, Elise N. Mariner, "Effect of dynamic loading on the frictional response of bovine articular cartilage", Journal of Biomechanics, 2005, 1665–1673.

[32] Chun-Yuh Huang, Anna Stankiewicz, "Anisotropy, inhomogeneity, andtension–compression nonlinearity of human glenohumeral cartilage in finite deformation", Journal of Biomechanics, 2005, 799–809.

[33] Oliver K. Erne, John B. Reid, "Depth-dependent strain of patellofemoral articular cartilage in unconfined compression". Journal of Biomechanics, 2005, 667–672.

[34] L.P. Li, W. Herzog, Strain-rate dependence of cartilage stiffness in unconfined compression: the role of fibril reinforcement versus tissue volume change in fluid pressurization Journal of Biomechanics, 2004, 375–382.

[35] W. Johannessen, J. M. CLOYD, "Trans-Endplate Nucleotomy Increases Deformation and Creep Response in Axial Loading", Annals of Biomedical Engineering, 2006, 687–696.

[36] James C. Iatridis, Jeffrey J. MacLean, "Mechanical damage to the intervertebral disc annulus fibrosus subjected to tensile loading", Journal of Biomechanics, 2005, 557–565.

[37] Daniel H.K. Chow a, Keith D.K. Luk, "Multi-planar bending properties of lumbar intervertebral joints following cyclic bending", Clinical Biomechanics, 2004, 99–106.

[38] V.R. Yingling, "Dynamic loading affects the mechanical properties and failure site of porcine spines, Clinical Biomechanics", 1997, 301-305.

[39] Thomas H. Jansen, Denis J. DiAngelo, "Computer Simulation Studies of Cervical Spine Extension Mechanics", IEEE, 1997.

[40] Congo T.S. Ching a, Daniel H.K. Chow, "The effect of cyclic compression on the mechanical properties of the inter-vertebral disc: An in vivo study in a rat tail model", Clinical Biomechanics,2003, 182–189.

[41] Kenneth R. Gratz, Van W. Wong, "Biomechanical assessment of tissue retrieved

after in vivo cartilage defect repair:tensile modulus of repair tissue and integration with host cartilage", Journal of Biomechanics, 2006, 138–146.

[42] Robin C. Evans, "Solute diffusivity correlates with mechanical properties and matrix density of compressed articular cartilage", Archives of Biochemistry and Biophysics, 2005, 1–10.

[43] E. Tanakaa, M. Tanakab, "Viscoelastic properties of canine temporomandibular joint disc in compressive load-relaxation", Archives of Oral Biology 44,1999 1021-1026.

[44] Jeffrey C. Wang, MD, J. Michael Kabo, Jeffrey C. Wang, MD, J. Michael Kabo, "The effect of uniform heating on the biomechanical properties of the intervertebral disc in a porcine model", The Spine Journal 5, 2005, 64–70.

[45] David Spenciner, PE, ScM, David Greene, "The multidirectional bending properties of the human lumbar intervertebral disc", The Spine Journal 6, 2006 248–257.

[46] H. C. Wu, R. F. Yao, "Mechanical Behavior of the Human Annulus Fibrosus", J. Biomechannics, Vol.9, 1987, 563–570.

[47] H. Weinans, J. Homminga, "Effects of Intervertebral Disc Bahavior on the Load Distribution and Fracture Risk of the Vertebral Body", Proceedings - 19th International Conference - IEEE/EMBS, 1997, 1865-1867.

[48] Luzhong Yin, Dawn M. Elliott, "A homogenization model of the annulus fibrosus", Journal of Biomechanics 38, 2005, 1674–1684.

[49] A. Shirazi-Adl and Harcharan Singh Ram,"3-D Finite Element Modeling of Human Spinal Discs and Correlation with Volume-Pressure Relation Due to Loading", IEEE, 1997, 1865-1867.

[50] Jun Yao, Sergio R Turteltaub, "A three-dimensional nonlinear finite element analysis of the mechanical behavior of tissue engineered intervertebral discs under complex loads", Biomaterials 27, 2006, 377–387.

[51] Hung-Wen Wei a, Shih-Sheng Sunb, "The influence of mechanical properties of subchondral plate, femoral head and neck on dynamic stress distribution of the articular cartilage", Medical Engineering & Physics 27, 2005, 295–304.

[52] Delphine Pe´rie´, David Korda, James C. Iatridis "Confined compression experiments on bovine nucleus pulposus and annulus fibrosus: sensitivity of the experiment in the determination of compressive modulus and hydraulic permeability", Journal of Biomechanics 38, 2005, 2164–2171.

[53] Robin C. Evans, Thomas M. Quinn "Solute diffusivity correlates with mechanical properties and matrix density of compressed articular cartilage" Archives of Biochemistry and Biophysics 442, 2005, 1–10.

[54] L. Y. Lum, N. L.C. Cher, C. G. Williams, and J. H. Elisseeff "An Extracellular Matrix Extract for Tissue-Engineered Cartilage", IEEE Engineering in Medicine and Biology Magazine, 2003, 71-76.

[55] F. Guilak, L. G. Alexopoulos, H. P. T. Beall and L. A. Setton, "Pericellular Matrix: Micropipette Aspiration of Canine Chondrons Isolated by Cartilage Homogenization" Annals of Biomedical Engineering, 2005, 1312-1315.

[56] F. Guilak, L. G. Alexopoulos, H. P. T. Beall and L. A. Setton, "Zonal Uniformity in Mechanical Properties of the Chondrocyte Pericellular Matrix: Micropipette Aspiration of Canine Chondrons Isolated by Cartilage Homogenization", Annals of Biomedical Engineering, 2005, 1312–1318.

[57] <http://www.cfsan.fda.gov/~ebam/r59.html> 2 Dec. 2006.

[58] A.J. M. Spencer, Continuum Mechanics, 1990, John Wiley and Sons.

[59] Yagonandan N., Kumaresan S., Pintar F., "Finite Element Model of the Human Lower Cervical Spine, Parametric Analysis of the C4-C6 unit", J. Biomechanical Engineering, 1997, 87-92.

[60] Goel V. K., Clausen J. D., "Prediction of load sharing among spinal components of a C5-C6 motion segment using the finite element approach", Spine, 1998, 684-691.

[61] S. P. Moroney, A. B. Schults, J. A. A. Miller and G. B. J. Andersson, "Load Displacement Properties of Lower Cervical Spine Motion Segments", BiomechanVicosl, 1998, 769-7791.